

Scrambling in the Quantum Lifshitz Model

Eugeniu Plamadeala and Eduardo Fradkin

Department of Physics and Institute for Condensed Matter Theory, University of Illinois at Urbana-Champaign, 1110 West Green Street, Urbana, Illinois 61801-3080, USA

Abstract. We study signatures of chaos in the quantum Lifshitz model through out-of-time ordered correlators (OTOC) of current operators. This model is a free scalar field theory with dynamical critical exponent $z = 2$. It describes the quantum phase transition in 2D systems, such as quantum dimer models, between a phase with an uniform ground state to another one with a spontaneously translation invariance. At the lowest temperatures the chaotic dynamics are dominated by a marginally irrelevant operator which induces a temperature dependent stiffness term. The numerical computations of OTOC exhibit a non-zero Lyapunov exponent (LE) in a wide range of temperatures and interaction strengths. The LE (in units of temperature) is a weakly temperature-dependent function; it vanishes at weak interaction and saturates for strong interaction. The Butterfly velocity increases monotonically with interaction strength in the studied region while remaining smaller than the interaction-induced velocity/stiffness.

1. Introduction

Scrambling is the delocalization of initially local quantum information over the entire system. It implies that information about the initial state cannot be deduced by any local measurements of the final state. This notion is closely related to the notion of quantum chaos in many-body systems[1]. The so-called out-of-time-order correlators were invented to capture the failure of semiclassical methods in a study of superconductivity.[2] More recently it has been realized that they are a way to quantify chaos and information scrambling in black holes [3, 4, 5]. Specifically, for generic local Hermitean operators W and V , the signature of chaos is a regime of exponential growth of the OTOC $C(t) \sim e^{\lambda t}$ after local relaxation has occurred but before the scrambling time when $C(t) \sim 1$. The exponent λ is called a “Lyapunov exponent” by analogy with the Lyapunov exponents of classical dynamical systems:[6, 7] in both classical and quantum cases the system loses memory of its initial state exponentially fast. It is generally conjectured that systems with this behavior are “chaotic”. In the classical setting this means that the system over very long times eventually explores all its available phase state with probability 1. Although the precise definition of chaos is lacking (or rather there is an abundance of them[1]), in the quantum setting of a chaotic system it is believed that, at times long compared with the scrambling time, the system becomes described by a density matrix and in some sense has thermalized.[8] The out-of-time ordered correlator $C(t)$ (OTOC) of two hermitian operators V and W is

$$C(t) = \text{tr}\{\rho[W(t), V]^\dagger[W(t), V]\} \quad (1.1)$$

Numerous works have recently studied quantum chaos both at strong[9, 3] and weak coupling,[10, 11] in gapped phases, in rational CFTs,[12, 13] and in strongly disordered phases.[14, 15, 16]

In this paper we will compute the chaos (Lyapunov) exponents and the Butterfly velocity for a system close to a quantum critical point. In general, this is a challenging problem since most quantum critical points are associated to a non-trivial UV fixed point of a quantum field theory. However in 2+1 dimensions there is a quantum critical theory, the quantum Lifshitz model [17] (qLM), which is a free (compactified) scalar field theory with dynamical exponent $z = 2$. Since this fixed point theory is a free field, it is not chaotic. In spite of its simplicity, the qLM is a non trivial theory with a rich spectrum of operators, and has been studied quite extensively.[17, 18, 19] One aspect of this theory that is useful in this context is that it has a marginally irrelevant operator[18, 20, 21] which, if included in the Lagrangian, spoils the integrability of the fixed point theory. This is thus a controlled setting to examine the behavior of the OTOCs of this theory within a perturbative approach.

The imaginary-time action of the qLM in 2+1-dimensions is:

$$S_0 = \frac{1}{2} \int d\tau d^2x \left((\partial_\tau \phi)^2 + \kappa (\nabla^2 \phi)^2 \right) \quad (1.2)$$

There are several variations of this model: the compactified and non-compactified real scalar, as well as the complex scalar. The leading irrelevant operator at all these critical points is the same - $(\nabla \phi)^4$, and for this reason we believe the physics concerning chaos will be *qualitatively* the same. For simplicity, here we choose to study the case of the non-compactified real scalar theory.

Since this QCP is described by a quadratic action, it is integrable and cannot thermalize. Lack of integrability is not sufficient to guarantee thermalization.[22] The

$(\nabla\phi)^4$ interaction is meant to both break integrability[23] and lead to thermalization, although we have no proof it does this. It is marginally irrelevant at the QCP and, barring $\cos(n\phi)$ terms only allowed (but less relevant at $\kappa \ll 1$) in the compactified theory, it is the the leading perturbation to the scaling form of the action. As with other irrelevant operators, its main effect is to shift the location of the QCP by inducing a renormalized stiffness, the coefficient of the relevant operator $(\nabla\phi)^2$, whose renormalized value is tuned to zero at $T = 0$ (but *not* at $T > 0$) as the definition of the QCP. Thus, our approach consists of deforming S_0 by the following:

$$S' = \int d\tau d^2x \left[r_{qc} (\nabla\phi)^2 + \frac{u}{4} (\nabla\phi)^4 \right] \quad (1.3)$$

where the stiffness $r_{qc} = r_{qc}(u)$ is chosen such that we hit the QCP as $T \rightarrow 0$ keeping the bare value of u fixed. The field ϕ is non-compact.

In order to perform a controlled calculation we choose to consider an N -flavor version of this model:

$$\mathcal{L}_{QLM,N} = \sum_a \frac{1}{2} [(\partial_\tau \phi_a)^2 + r_{qc} (\nabla\phi_a)^2 + \kappa (\nabla^2 \phi_a)^2] + \frac{u}{4N} \sum_{a,b} (\nabla\phi_a)^2 (\nabla\phi_b)^2 \quad (1.4)$$

Furthermore it is helpful to rewrite the $(\nabla\phi)^4$ term by introducing an auxiliary field σ through a Hubbard-Stratonovich transformation:

$$Z_E = \int \mathcal{D}\phi e^{-S_{QLM,N}[\phi]} = \int \mathcal{D}\phi \mathcal{D}\sigma e^{-S_N[\phi,\sigma]} \quad (1.5)$$

In this form the (Euclidean) Lagrangian is

$$\mathcal{L}_N[\phi,\sigma] = \sum_a \frac{1}{2} [(\partial_\tau \phi_a)^2 + r_{qc} (\nabla\phi_a)^2 + \kappa (\nabla^2 \phi_a)^2] - \frac{\sigma^2}{4u} + \frac{\sigma}{2\sqrt{N}} \sum_a (\nabla\phi_a)^2 \quad (1.6)$$

As discussed in Appendix Appendix A, at $N = \infty$ we can solve the theory most naturally by introducing a new coupling:

$$r_{\text{eff}} = \frac{\langle\sigma\rangle}{\sqrt{N}} + r_{qc} \quad \text{where} \quad r_{\text{eff}} = \frac{uT}{4\pi\kappa} \frac{\ln\left(\frac{\sqrt{\kappa}T}{r_{\text{eff}}}\right)}{1 + \frac{u}{16\pi\kappa^{3/2}} \left[\ln\left(\frac{4\kappa\Lambda^2}{r_{\text{eff}}}\right) \right]} \quad (1.7)$$

We note that the expectation value of the auxiliary field $\langle\sigma\rangle$ induces a stiffness (“velocity”) for the ϕ field (instead of a “thermal mass” as in ϕ^4 theory). We now discuss solutions of the equation above.

At fixed interaction strength u and sufficiently low temperatures the logarithm dominates the denominator and we obtain (see discussion around EqnA.12)

$$r_{\text{eff}} \approx 4T\sqrt{\kappa} \frac{\ln \ln\left(\frac{\Lambda^2}{T\sqrt{\kappa}}\right)}{\ln\left(\frac{\Lambda^2}{T\sqrt{\kappa}}\right)} \quad (1.8)$$

which is consistent with our assumptions at low T . The marginality of the $(\nabla\phi)^4$ term has induced log corrections that violate $z = 2$ scaling. Note that r_{eff} appears to be independent of the interaction strength u at low T . This is only true when the approximation we made in the denominator holds: $\frac{u}{16\pi\kappa^{3/2}} \left[\ln\left(\frac{4\kappa\Lambda^2}{r_{\text{eff}}}\right) \right] \gg 1$. The

assumption we began with is clearly valid. We will call this the *low temperature regime*. On the other hand at higher temperatures or small u the opposite is true

$$\frac{u}{16\pi\kappa^{3/2}} \left[\ln \left(\frac{4\kappa\Lambda^2}{r_{\text{eff}}} \right) \right] \ll 1 \quad (1.9)$$

and using similar methods we obtain a different saddle-point equation

$$r_{\text{eff}} = \frac{uT}{4\pi\kappa} \ln \left(\frac{\sqrt{\kappa}T}{r_{\text{eff}}} \right) \quad \text{with solution} \quad r_{\text{eff}} = \sqrt{\kappa}T \left(\frac{u}{4\pi\kappa^{3/2}} \right) \ln \left(\frac{4\pi\kappa^{3/2}}{u} \right) \quad (1.10)$$

We call this the *weak interaction regime*. We will study both regimes simultaneously by defining $\alpha(u, T) = r_{\text{eff}}(u, T)/T$. Since α has very weak temperature dependence in both regimes, we will often treat α as an independent parameter (in a wide but finite range of temperatures).

The $1/N$ corrections are then captured by the following action (see Appendix B) where the λ field is the deviation from the saddle-point value of σ , i.e. $\lambda = \sigma - \langle \sigma \rangle_{N=\infty}$,

$$\mathcal{L}_{\phi, \lambda, N} = \sum_a \frac{1}{2} [(\partial_\tau \phi_a)^2 + r_{\text{eff}}(\nabla \phi_a)^2 + \kappa(\nabla^2 \phi_a)^2] - \frac{\lambda^2}{4u} + \frac{\lambda}{2\sqrt{N}} \sum_a (\nabla \phi_a)^2 \quad (1.11)$$

At leading order in N the ϕ_a fields decouple from λ and each other, and there is no chaos. Therefore, the chaos (Lyapunov) exponent is at most of order $1/N$ at large N and we must study $1/N$ corrections using the theory of Eq.1.11.

The building blocks of our perturbative expansions are the imaginary-time ϕ_a propagator

$$\mathcal{G}(\tau, \mathbf{x}) \delta_{a,b} = \langle T_\tau \phi_a(\tau, \mathbf{x}) \phi_b(0, 0) \rangle \quad (1.12)$$

$$\mathcal{G}(i\omega_n, \mathbf{q}) = \frac{1}{\omega_n^2 + \epsilon_q^2}, \quad \text{where} \quad \epsilon_q^2 = r_{\text{eff}}(u, T) \mathbf{q}^2 + \kappa \mathbf{q}^4 \quad (1.13)$$

The retarded ϕ_a propagator $\mathcal{G}_R(\omega, \mathbf{k})$ is obtained as usual by analytic continuation $i\omega_n \rightarrow \omega + i0$. The spectral function is

$$A(\omega, \mathbf{k}) = -2\Im \mathcal{G}_R(\omega, \mathbf{k}) = \frac{\pi}{\epsilon_{\mathbf{k}}} [\delta(\omega - \epsilon_{\mathbf{k}}) - \delta(\omega + \epsilon_{\mathbf{k}})] \quad (1.14)$$

We will also make use of the symmetrized Wightman propagator of the ϕ fields, defined as

$$\mathcal{G}_W(t, \mathbf{x}) \delta_{a,b} = \text{tr} \{ \rho^{1/2} \phi_a(\mathbf{x}, t) \rho^{1/2} \phi_b(0) \} \quad (1.15)$$

By manipulations similar to those in Appendix C of Ref.[[11]] the Wightman propagator can be related to the spectral function through

$$\mathcal{G}_W(\omega, \mathbf{k}) = \frac{A(\omega, \mathbf{k})}{2 \sinh \frac{\beta\omega}{2}} \quad (1.16)$$

We will shortly need the ϕ and λ propagators dressed to leading order. We denote the bare λ field propagator as $\mathcal{G}_\lambda^0(\tau, \mathbf{x}) = -2u$. It picks up a $O(N^0)$ correction through its self-energy $\Pi(i\omega_n, \mathbf{q})$ to give the dressed λ propagator

$$\mathcal{G}_\lambda(i\omega_n, \mathbf{q}) = \frac{1}{\frac{1}{-2u} - \Pi(i\omega_n, \mathbf{q})} \quad (1.17)$$

from which one can derive the other functions:

$$\text{the retarded propagator} \quad \mathcal{G}_{R,\lambda}(\omega, \mathbf{q}) = -\mathcal{G}_\lambda(i\omega_n \rightarrow \omega + i0, \mathbf{q}) \quad (1.18)$$

$$\text{the spectral function} \quad A_\lambda(\omega, \mathbf{q}) = -2\Im \mathcal{G}_{R,\lambda}(\omega, \mathbf{q}) \quad (1.19)$$

$$\text{the Wightman propagator} \quad \mathcal{G}_{W,\lambda}(\omega, \mathbf{q}) = \frac{A_\lambda(\omega, \mathbf{q})}{2 \sinh \frac{\beta\omega}{2}} \quad (1.20)$$

The Feynman rule for the $\phi - \lambda$ vertex follows from

$$-\mathcal{L}_E \propto \frac{1}{2\sqrt{N}} \int_{\omega_n, \omega_m} \int_{\mathbf{k}, \mathbf{q}} (-\mathbf{k} \cdot \mathbf{q}) \lambda(-i\omega_n - i\omega_m, -\mathbf{k} - \mathbf{q}) \phi_a(i\omega_n, \mathbf{k}) \phi_a(i\omega_m, \mathbf{q}) \quad (1.21)$$

Here and below we use the notation $\int_{\mathbf{p}} = \int \frac{d^2 p}{(2\pi)^2}$ and $\int_{\omega_n} = T \sum_{\omega_n}$. The vertex then equals $\frac{-\mathbf{k}_1 \cdot \mathbf{k}_2}{\sqrt{N}} \delta(\sum_i \mathbf{k}_i)$, where the dotted momenta belong to the ϕ fields.

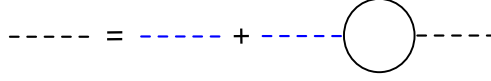


Figure 1. The self-energy correction of the λ field at leading order in $1/N$.

The one-loop self-energy $\Pi(i\omega_n, \mathbf{q})$ of the λ field comes from the Dyson equation for the field λ , the Feynman diagram shown in Fig.1 and equals

$$\Pi(i\omega_n, \mathbf{q}) = \frac{T}{2} \sum_{\nu_n} \int_{\mathbf{k}}^{\Lambda} \frac{(\mathbf{k} \cdot (\mathbf{k} + \mathbf{q}))^2}{(\nu_n + \omega_n)^2 + \epsilon_{\mathbf{k}+\mathbf{q}}^2} \frac{1}{\nu_n^2 + \epsilon_{\mathbf{k}}^2} \quad (1.22)$$

where the factor of $1/2$ comes from combinatorics ($1/2$ from second order of exponential series, and two factors from vertex; on top there are two ways to contract the ϕ 's, and two to contract the λ 's). In Appendix D we discuss the computation of this object, which must ultimately be done numerically.

Similarly, the one-loop self-energy of ϕ is given by the Feynman diagrams:

$$\Sigma(i\omega_n, \mathbf{q}) = \text{---} \text{---} \text{---} \text{---} + \text{---} \text{---} \text{---} \text{---} \quad (1.23)$$

The second diagram in Eq.(1.23) induces only a real shift of the pole and plays no role in our calculation.

$$\Sigma(i\omega_n, \mathbf{q}) = \frac{T}{N} \sum_{\nu_n} \int_{\mathbf{k}}^{\Lambda} (\mathbf{q} \cdot (\mathbf{q} + \mathbf{k}))^2 \mathcal{G}(i\omega_n + i\nu_n, \mathbf{q} + \mathbf{k}) \mathcal{G}_\lambda(i\nu_n, \mathbf{k}) \quad (1.24)$$

where \mathcal{G}_λ is already one-loop corrected. This object is computed in Appendix E. Note that the second diagram also contributes at order $1/N$ but as it induces only a real shift of the pole we drop it with the philosophy that the location of the pole is a physical quantity that we choose to keep fixed with a suitable counterterm.

2. Perturbative expansion of OTOC

Instead of studying the OTOC of Eq.1.1 we will study a closely related object with the same growth properties. Following the approach employed for matrix ϕ^4 theory in the large N limit by Stanford[10], we shift half the fields half-way along the thermal circle.[11] This removes spurious short-distance divergences of coincident operators, without modifying the exponential growth. The resulting operators insertions in complex time lie on the contour shown in Fig. 2.

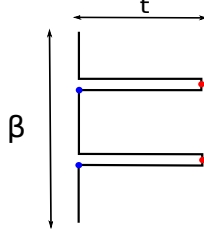


Figure 2. Complex time contour of the operators insertions of the regulated OTOC. The blue (red) dot corresponds to the $V(0)$ ($W(t)$) operator.

Specifically we choose to study the following (regulated) OTOC

$$C(t_1 - t_2, \mathbf{x}_1 - \mathbf{x}_2) = -\frac{1}{N^2} \sum_{a,b} \text{Tr} \{ \sqrt{\rho} [\nabla \phi_a(\mathbf{x}_1, t_1), \nabla \phi_b(\mathbf{x}_2, t_2)] \sqrt{\rho} [\nabla \phi_a(\mathbf{x}_1, t_1), \nabla \phi_b(\mathbf{x}_2, t_2)] \} \quad (2.1)$$

Note that gradients are dotted into each other within each commutator. The OTOC can be expanded in powers of the interaction vertex.

We derive the rules in Appendix C (they are almost identical to those in Chowdhury and Swingle [11]), and simply present them here:

- (i) Vertex insertions can occur on either time-fold. Each comes with a factor of $\frac{-i\mathbf{k}_1 \cdot \mathbf{k}_2}{2\sqrt{N}} \delta_{ab}$ (coming from ϕ_a, ϕ_b). Contractions inside each time fold represent self-energy corrections and are counted separately.
- (ii) Horizontal lines correspond to retarded propagators $i\mathcal{G}_R, i\mathcal{G}_{R,\lambda}$, vertical lines to Wightman propagators $G_W, G_{W,\lambda}$.
- (iii) Each line must be directed, left to right or top to down. This determines whether a momentum/frequency is incoming or outgoing. The sum of incoming must equal sum of outgoing at each vertex.



Figure 3. The simplest ladder diagram with rungs of type 1, $C_1(\nu, \mathbf{q} = 0)$ defined in Eq.2.2.

There are two classes of diagrams then that are most important, both involve contractions between the different time folds. The first class involve ladder rungs of

λ propagators (we will call them type 1). The simplest example of a type 1 diagram is shown in Fig.2.

Its value at $\mathbf{q} = 0$ momentum transfer is

$$C_1(\nu, \mathbf{q} = 0) = \frac{1}{N^2} \int_{\mathbf{p}, \mathbf{p}'} (\mathbf{p} \cdot \mathbf{p}')^4 \int_{\omega, \omega'} \mathcal{G}_R(\mathbf{p}, \omega) \mathcal{G}_R(-\mathbf{p}, \nu - \omega) \mathcal{G}_\lambda^W(\mathbf{p} - \mathbf{p}', \omega - \omega') \\ \times \mathcal{G}_R(\mathbf{p}', \omega') \mathcal{G}_R(-\mathbf{p}', \nu - \omega') \quad (2.2)$$

For clarity and conciseness, in Eq.2.2 we present the expression at $\mathbf{q} = 0$. The full expression for $C_1(\nu, \mathbf{q})$ is worked out in Appendix C.

An example of the second class of diagrams is shown in Fig.2. These involve ladder rungs of ϕ propagators (we will call them type 2). The expression for the simplest such diagram is

$$C_2(\nu, \mathbf{q} = 0) = \frac{1}{N^2} \int_{\mathbf{p}, \mathbf{p}'} (\mathbf{p} \cdot \mathbf{p}')^2 \int_{\omega, \omega'} \mathcal{G}_R(\nu - \omega, -\mathbf{p}) \mathcal{G}_R(\omega, \mathbf{p}) \mathcal{G}_{\text{eff}}(\nu, \mathbf{q}; \omega', \omega, \mathbf{p}', \mathbf{p}) \\ \times \mathcal{G}_R(\nu - \omega', -\mathbf{p}') \mathcal{G}_R(\omega', \mathbf{p}') \quad (2.3)$$

where \mathcal{G}_{eff} above represents the loop of four propagators that form the inner rectangle in Fig 2. It is given by

$$\mathcal{G}_{\text{eff}}(\nu, \mathbf{q} = 0; \omega', \omega, \mathbf{p}', \mathbf{p}) = \int_{\omega'', \mathbf{p}''} (\mathbf{p} \cdot (\mathbf{p}'' - \mathbf{p}))^2 (\mathbf{p}' \cdot (\mathbf{p}' - \mathbf{p}''))^2 \\ \times \mathcal{G}_W(\omega'' - \omega, \mathbf{p}'' - \mathbf{p}) \mathcal{G}_W(\omega' - \omega'', \mathbf{p}' - \mathbf{p}'') \\ \times \mathcal{G}_{R,\lambda}(\nu - \omega'', -\mathbf{p}'') \mathcal{G}_{R,\lambda}(\omega'', \mathbf{p}'') \quad (2.4)$$

The functions \mathcal{G}_W and $\mathcal{G}_{R,\lambda}$ are defined in Eqns 1.16 and 1.18. In the sequel, we will typically suppress the ν and \mathbf{q} dependence of \mathcal{G}_{eff} and consider it implicit.



Figure 4. The simplest ladder diagram with rungs of type 2, $C_2(\nu, \mathbf{q} = 0)$ defined in Eq.2.3.

At late times both C_1 and C_2 contribute at order t/N^2 . A general diagram with n_1 rungs of type 1 and n_2 rungs of type 2 is of order $1/N^{n_1+n_2+1}$, so we expect their sum to be of order $1/N$. We ignored crossed diagrams because they are parametrically smaller than the ladder diagrams (see Appendix C.1).

3. Computation of the OTOC and the Bethe-Salpeter Equation

Before we compute the OTOC, $\mathcal{C}(t) = \int d^2x \mathcal{C}(t, \mathbf{x})$, we will briefly describe the structure of the calculation.

Instead of aiming directly for $\mathcal{C}(t, \mathbf{x})$ we will obtain $\mathcal{C}(\nu, \mathbf{q})$, which is its Laplace transform in frequency and the Fourier transform in momentum. The $\mathbf{q} = 0$ value is sufficient to compute the Lyapunov exponent λ_L , while the $\mathbf{q} \neq 0$ value is necessary to obtain the Butterfly velocity (and a semi-independent verification of λ_L).

The function $\mathcal{C}(\nu, \mathbf{q})$ has a diagrammatic expansion in powers of $1/N$. The first two terms are $\mathcal{C}_1(\nu, \mathbf{q})$ and $\mathcal{C}_2(\nu, \mathbf{q})$ previously defined in Eqns 2.2 and 2.3 corresponding to diagrams with rungs of type 1 and 2 respectively. We will set up and solve the Bethe-Salpeter equation for $\mathcal{C}(\nu, \mathbf{q})$ in terms of an auxiliary function $g(\nu, \mathbf{q}; \omega, \mathbf{p})$ defined by

$$\mathcal{C}(\nu, \mathbf{q}) = \frac{1}{N} \int \frac{d\omega}{2\pi} \int_{\mathbf{p}} \mathbf{p}^2 g(\nu, \mathbf{q}; \omega, \mathbf{p}), \quad (3.1)$$

The Bethe-Salpeter equation will be finally recast to an integral equation, which we will need to solve numerically. To do that we will discretize and turn it into a matrix eigenvalue problem. Finally the eigenvalue with the largest positive real part will dominate the exponential growth of the OTOC in time.

We study the $\mathbf{q} = 0$ case first. We subsequently suppress the \mathbf{q} index (when zero) and write $\mathcal{C}(\nu)$ in place of $\mathcal{C}(\nu, \mathbf{q})$. To compute the OTOC $\mathcal{C}(\nu)$ we now proceed with an evaluation of the sum of ladder diagrams of Fig.3.

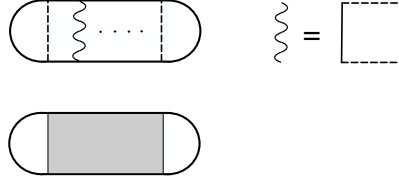


Figure 5. Top left is a general uncrossed diagram. The bottom represents the complete sum $\mathcal{C}(\nu)$.

To this end we set up a Bethe-Salpeter equation, which diagrammatically is represented in figure Fig.3. We write down the value of the first few diagrams with

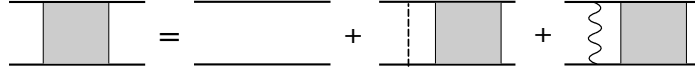


Figure 6. A diagrammatic definition of the Bethe-Salpeter equation for $\mathcal{C}(t)$.

rungs of type 1:

$$\mathcal{C}(\nu) = \frac{1}{N} \int_{\omega, \mathbf{p}} \mathbf{p}^4 \mathcal{G}_R(\nu - \omega, -\mathbf{p}) \mathcal{G}_R(\omega, \mathbf{p}) \quad (3.2)$$

$$+ \frac{1}{N^2} \int_{\omega, \omega', \mathbf{p}, \mathbf{p}'} \mathbf{p}^2 \mathcal{G}_R(\nu - \omega, -\mathbf{p}) \mathcal{G}_R(\omega, \mathbf{p}) (\mathbf{p} \cdot \mathbf{p}')^2 \mathcal{G}_{W, \lambda}(\omega' - \omega, \mathbf{p}' - \mathbf{p}) \times \mathcal{G}_R(\nu - \omega', -\mathbf{p}') \mathcal{G}_R(\omega', \mathbf{p}') \mathbf{p}'^2 \quad (3.3)$$

$$+ \frac{1}{N^3} \int \mathbf{p}^2 (\mathbf{p} \cdot \mathbf{p}')^2 (\mathbf{p}' \cdot \mathbf{p}'')^2 (\mathbf{p}'')^2 G_{\mathbf{p}}^2 \mathcal{G}_{W, \lambda} G_{\mathbf{p}'}^2 \mathcal{G}_{W, \lambda} G_{\mathbf{p}''}^2 + \dots \quad (3.4)$$

where the last line is written schematically. This allows us to infer the Bethe-Salpeter equation for $\mathcal{C}(\nu)$, written in terms of the auxiliary function g :

$$g(\nu; \omega, \mathbf{p}) = \mathcal{G}_R(\nu - \omega, -\mathbf{p}) \mathcal{G}_R(\omega, \mathbf{p}) \times \left[\mathbf{p}^2 + \frac{1}{N} \int_{\omega', \mathbf{p}'} (\mathbf{p} \cdot \mathbf{p}')^2 \mathcal{G}_{W, \lambda}(\omega' - \omega, \mathbf{p}' - \mathbf{p}) g(\nu; \omega', \mathbf{p}') \right] \quad (3.5)$$

We can also include the type 2 rungs by making the following replacement in the expression given above

$$(\mathbf{p} \cdot \mathbf{p}')^2 \mathcal{G}_{W,\lambda}(\omega' - \omega, \mathbf{p}' - \mathbf{p}) \rightarrow (\mathbf{p} \cdot \mathbf{p}')^2 \mathcal{G}_{W,\lambda}(\omega' - \omega, \mathbf{p}' - \mathbf{p}) + \mathcal{G}_{\text{eff}}(\nu, \mathbf{q} = 0; \omega', \omega; \mathbf{p}', \mathbf{p})$$

where \mathcal{G}_{eff} is given by Eq.2.4.

To make progress and extract the leading time-dependence we must simplify the object $\mathcal{G}_R(\nu - \omega, -\mathbf{p})\mathcal{G}_R(\omega, \mathbf{p})$. We do this by the following replacement:

$$\mathcal{G}_R(\nu - \omega, -\mathbf{p})\mathcal{G}_R(\omega, \mathbf{p}) \rightarrow \frac{\pi i}{\epsilon_{\mathbf{p}}} \frac{\delta(\omega^2 - \epsilon_{\mathbf{p}}^2)}{\nu + i2\Gamma_{\mathbf{p}}} \quad (3.6)$$

As explained in Appendix C.2 this replacement achieves three things: it simplifies the expression, it captures the pole structure that leads to leading late-time dependence in $\mathcal{C}(t)$, and finally it also captures the scattering rate, $\Gamma_{\mathbf{p}}$, of the ϕ fields (see discussion around Eqn.C.29).

Since the product of the two Green functions \mathcal{G}_R has an on-shell delta function condition, we choose the following ansatz

$$g(\nu; \omega, \mathbf{p}) = g(\nu; \mathbf{p})\delta(\omega^2 - \epsilon_{\mathbf{p}}^2) \quad (3.7)$$

This simplifies the Bethe-Salpeter equation 3.5 to the following

$$-i\nu g(\nu; \mathbf{p}) = \frac{\pi \mathbf{p}^2}{\epsilon_{\mathbf{p}}} + \frac{1}{N} \int_{\mathbf{l}} \left(\mathcal{R}_1(\mathbf{l}, \mathbf{p}) + \mathcal{R}_2(\mathbf{l}, \mathbf{p}) - 2N\Gamma_{\mathbf{p}} \delta^{(2)}(\mathbf{l} - \mathbf{p}) \right) g(\nu; \mathbf{l}) \quad (3.8)$$

where we introduce auxiliary functions $\mathcal{R}_1, \mathcal{R}_2$ to compactify the expression. They are given by

$$\mathcal{R}_1(\mathbf{l}, \mathbf{p}) = \mathcal{R}_{1,+}(\mathbf{l}, \mathbf{p}) + \mathcal{R}_{1,-}(\mathbf{l}, \mathbf{p}) \quad (3.9)$$

$$\mathcal{R}_{1,\pm}(\mathbf{l}, \mathbf{p}) = \frac{(\mathbf{l} \cdot \mathbf{p})^2}{4\epsilon_{\mathbf{l}}\epsilon_{\mathbf{p}}} \mathcal{G}_{W,\lambda}(\pm\epsilon_{\mathbf{l}} - \epsilon_{\mathbf{p}}, \mathbf{l} - \mathbf{p}) \quad (3.10)$$

$$\mathcal{R}_2(\mathbf{l}, \mathbf{p}) = \mathcal{R}_{2,+}(\mathbf{l}, \mathbf{p}) + \mathcal{R}_{2,-}(\mathbf{l}, \mathbf{p}) \quad (3.11)$$

$$\mathcal{R}_{2,\pm}(\mathbf{l}, \mathbf{p}) = \frac{1}{4\epsilon_{\mathbf{l}}\epsilon_{\mathbf{p}}} \mathcal{G}_{\text{eff}} \left(\pm\epsilon_{\mathbf{l}}, \epsilon_{\mathbf{p}}; \mathbf{l} - \mathbf{p}, \frac{\mathbf{l} + \mathbf{p}}{2} \right) \quad (3.12)$$

Note that $\mathcal{R}_{2,\pm}(\mathbf{l}, \mathbf{p})$ actually depends on ν, κ, u, T in addition to \mathbf{l}, \mathbf{p} . Similarly \mathcal{R}_1 depends on κ, u, T . We convinced ourselves numerically that indeed $\mathcal{R}_1(\mathbf{l}, \mathbf{l})$ vanishes. Both $\mathcal{R}_1(\mathbf{l}, \mathbf{p})$ and $\mathcal{R}_2(\mathbf{l}, \mathbf{p})$ also vanish when either $\mathbf{l}, \mathbf{p} \rightarrow 0$ due to the factors of momentum in the numerator.

4. Lyapunov Exponent and Butterfly velocity

We note that 3.8 can be made dimensionless by the replacement $\nu \rightarrow \nu T, \mathbf{p} \rightarrow \mathbf{p}\sqrt{T}, r_{\text{eff}}(u, T) = \alpha(u, T)T$, with $[g] = [1/T] = 2$. Then, by dimensional considerations and inspection of r_{eff} , the Lyapunov exponent λ_L will take the form

$$\lambda_L = n(u, \alpha(u, T)) \frac{T}{N} \quad (4.1)$$

where $n(u, \alpha(u, T))$ is a dimensionless function with the following behaviors

- In the *weak interaction regime* $n(u, T) = n(u)$ is temperature independent with $n(u = 0) = 0$ (since at $u = 0$ the model becomes integrable).
- In the *low temperature regime*, $n(u, T)$ inherits a weak temperature dependence from $\alpha(T)$.

We solve the integral equation of Eq.3.8 numerically. Given the eigenfunction $g_\eta(\nu; \mathbf{p})$ of the right-hand-side integral with eigenvalue η we obtain the following final form for 3.8:

$$-i\nu g_\eta(\nu; \mathbf{p}) = \frac{\pi \mathbf{p}^2}{\epsilon_{\mathbf{p}}} + \frac{\eta}{N} g_\eta(\nu; \mathbf{p}) \quad (4.2)$$

All the eigenvalues η we obtained numerically were complex; most had a negative real part which leads to exponential decay. We typically found only a handful of eigenvalues with a positive real part, and it is these that lead to exponential growth of chaotic correlations. An inverse Laplace transform $\mathcal{C}(t) = \int_\nu e^{-i\nu t} \mathcal{C}(\nu)$ then gives

$$\mathcal{C}(t) \sim e^{\eta t T/N} \quad (4.3)$$

which allows us to identify the eigenvalue η as the dimensionless function $n(u, T)$ introduced earlier in Eq.(4.1).

We remark that while maximal chaos is often associated with the absence of “quasiparticles” [24, 25] (so presumably large scattering rate Γ_p), in equation 3.8 the scattering rate appears to decrease the chaos exponent in an apparent contradiction. There is however no contradiction as $\mathcal{R}_1(\mathbf{l}, \mathbf{p})$ which is present in Eq.3.8 and contributes to chaos also contributes to $\Gamma_{\mathbf{p}}$ (see Eq.E.5).

Despite its $z = 2$ scaling, the quantum Lifshitz critical point has apriori a velocity scale $\sqrt{\kappa\Lambda}$. This is consistent with Lieb-Robinson type bounds that show the existence of a light cone even in non-relativistic systems.[26] This is explicitly a UV sensitive quantity. As we argued earlier a “thermal velocity”, $v = \sqrt{r(T)} \sim \sqrt{\alpha(u, T)T}$, is induced in our model close to the QCP.

There is growing evidence that OTOCs like ours propagate ballistically in systems that exhibit a non-zero chaos exponent.[27, 28]. Roberts and Swingle[29] have argued that the associated velocity is an effective Lieb-Robinson velocity in the IR, and is UV insensitive (although this depends on the considered operators, see supplemental material of Ref [29]). Multiple calculations support this conjecture[30].

In the qLM we find numerical evidence that $C(t, \mathbf{k})$ grows exponentially with an exponent

$$\lambda(\mathbf{k}) = \lambda_L - D_L \mathbf{k}^2 + \dots \quad (4.4)$$

where λ_L denotes the Lyapunov exponent. With some additional assumptions, that will be spelled out later, it follows that

$$C(t, \mathbf{x}) \sim \int_{\mathbf{k}} e^{i\mathbf{k} \cdot \mathbf{x}} e^{(\lambda_L - D_L \mathbf{k}^2)t} \sim e^{\lambda_L t - \frac{\mathbf{x}^2}{4D_L t}} \quad (4.5)$$

and the wavefront propagates ballistically with (by definition) Butterfly velocity $v_B = \sqrt{4D_L \lambda_L}$.

Mirroring the discussion for $\mathcal{C}(t)$, for $\mathbf{q} \neq 0$ we define the auxiliary function $g(\nu, \mathbf{q}; \omega, \mathbf{p})$

$$\mathcal{C}(\nu) = \frac{1}{N} \int \frac{d\omega}{2\pi} \int_{\mathbf{p}} \mathbf{p} \cdot (\mathbf{p} - \mathbf{q}) g(\nu, \mathbf{q}; \omega, \mathbf{p}) \quad (4.6)$$

and obtain the new Bethe-Salpeter equation for Type 1 ladders:

$$\begin{aligned} g(\nu, \mathbf{q}; \omega, \mathbf{p}) &= \mathcal{G}_R(\nu - \omega, \mathbf{q} - \mathbf{p}) \mathcal{G}_R(\omega, \mathbf{p}) \\ &\times \left[\mathbf{p} \cdot (\mathbf{p} - \mathbf{q}) + \frac{1}{N} \int_{\omega', \mathbf{p}'} (\mathbf{p} \cdot \mathbf{p}') (\mathbf{q} - \mathbf{p}) \cdot (\mathbf{q} - \mathbf{p}') \mathcal{G}_{W, \lambda}(\omega' - \omega, \mathbf{p}' - \mathbf{p}) g(\nu, \mathbf{q}; \omega', \mathbf{p}') \right] \end{aligned} \quad (4.7)$$

The Type 2 rungs are included by shifting

$$\begin{aligned} & (\mathbf{p} \cdot \mathbf{p}') (\mathbf{q} - \mathbf{p}) \cdot (\mathbf{q} - \mathbf{p}') \mathcal{G}_{W,\lambda}(\omega' - \omega, \mathbf{p}' - \mathbf{p}) \\ & \rightarrow (\mathbf{p} \cdot \mathbf{p}') (\mathbf{q} - \mathbf{p}) \cdot (\mathbf{q} - \mathbf{p}') \mathcal{G}_{W,\lambda}(\omega' - \omega, \mathbf{p}' - \mathbf{p}) + \mathcal{G}_{\text{eff}}(\nu, \mathbf{q}; \omega, \omega', \mathbf{p}, \mathbf{p}') \end{aligned} \quad (4.8)$$

where

$$\begin{aligned} \mathcal{G}_{\text{eff}}(\nu, \mathbf{q}; \omega, \omega', \mathbf{p}, \mathbf{p}') = & \int_{\omega'', \mathbf{p}''} (\mathbf{q} - \mathbf{p}) \cdot (\mathbf{p}'' - \mathbf{p}) \mathbf{p} \cdot (\mathbf{p}'' - \mathbf{p}) (\mathbf{q} - \mathbf{p}') \cdot (\mathbf{p}' - \mathbf{p}'') (\mathbf{p}' - \mathbf{p}'') \cdot \mathbf{p}' \\ & \times \mathcal{G}_W(\omega'' - \omega, \mathbf{p}'' - \mathbf{p}) \mathcal{G}_W(\omega' - \omega'', \mathbf{p}' - \mathbf{p}'') \mathcal{G}_{R,\lambda}(\nu - \omega'', \mathbf{q} - \mathbf{p}'') \mathcal{G}_{R,\lambda}(\omega'', \mathbf{p}'') \end{aligned} \quad (4.9)$$

A simplified expression for $\mathcal{G}_{\text{eff}}(\nu, \mathbf{q}; \omega, \omega', \mathbf{p}, \mathbf{p}')$ that is more amenable to numerical evaluation is provided in Eqn C.40.

Adopting the ansatz

$$g(\nu, \mathbf{q}; \omega, \mathbf{p}) = \frac{1}{2\epsilon_{\mathbf{p}}} [g_+(\mathbf{p})\delta(\omega - \epsilon_{\mathbf{p}}) + g_-(\mathbf{p})\delta(\omega + \epsilon_{\mathbf{p}})] \quad (4.10)$$

we arrive at the following system of integral equations

$$\begin{aligned} (-i\nu + i\delta\epsilon_{\mathbf{q}} + 2\Gamma_{\mathbf{p}}) g_+(\mathbf{p}) = & \frac{\pi}{\epsilon_{\mathbf{q}-\mathbf{p}}} \mathbf{p} \cdot (\mathbf{q} - \mathbf{p}) \\ & + \frac{1}{N} \int_{\mathbf{p}'} \mathcal{R}_+(\mathbf{p}', \mathbf{p}) g_+(\mathbf{p}') + \mathcal{R}_-(\mathbf{p}', \mathbf{p}) g_-(\mathbf{p}') \end{aligned} \quad (4.11)$$

$$\begin{aligned} (-i\nu - i\delta\epsilon_{\mathbf{q}} + 2\Gamma_{\mathbf{p}}) g_-(\mathbf{p}) = & \frac{\pi}{\epsilon_{\mathbf{q}-\mathbf{p}}} \mathbf{p} \cdot (\mathbf{q} - \mathbf{p}) \\ & + \frac{1}{N} \int_{\mathbf{p}'} \mathcal{R}_-(\mathbf{p}', \mathbf{p}) g_+(\mathbf{p}') + \mathcal{R}_+(\mathbf{p}', \mathbf{p}) g_-(\mathbf{p}') \end{aligned} \quad (4.12)$$

The integral kernels are almost identical to the earlier versions:

$$\mathcal{R}_{\pm}(\nu, \mathbf{q}; \mathbf{p}', \mathbf{p}) = R_{1,\pm}(\nu, \mathbf{q}; \mathbf{p}', \mathbf{p}) + R_{2,\pm}(\nu, \mathbf{q}; \mathbf{p}', \mathbf{p}) \quad (4.13)$$

$$\mathcal{R}_{1,\pm}(\nu, \mathbf{q}; \mathbf{l}, \mathbf{p}) = \frac{(\mathbf{q} - \mathbf{l}) \cdot (\mathbf{q} - \mathbf{p}) \mathbf{l} \cdot \mathbf{p}}{4\epsilon_{\mathbf{l}}\epsilon_{\mathbf{p}}} \mathcal{G}_{W,\lambda}(\pm\epsilon_{\mathbf{l}} - \epsilon_{\mathbf{p}}, \mathbf{l} - \mathbf{p}) \quad (4.14)$$

$$\mathcal{R}_{2,\pm}(\nu, \mathbf{q}; \mathbf{l}, \mathbf{p}) = \frac{1}{4\epsilon_{\mathbf{l}}\epsilon_{\mathbf{p}}} \mathcal{G}_{\text{eff}}\left(\nu, \mathbf{q}; \pm\epsilon_{\mathbf{l}}, \epsilon_{\mathbf{p}}; \mathbf{l} - \mathbf{p}, \frac{\mathbf{l} + \mathbf{p}}{2}\right) \quad (4.15)$$

We have made the following approximations in reaching the above expressions: $\epsilon_{\mathbf{p}'}\epsilon_{\mathbf{q}-\mathbf{p}} \approx \epsilon_{\mathbf{p}'}\epsilon_{\mathbf{p}}$, $\epsilon_{\mathbf{p}} - \epsilon_{\mathbf{q}-\mathbf{p}} \equiv \delta\epsilon_{\mathbf{q}} \approx \mathbf{q} \cdot \mathbf{v}_{\mathbf{p}}$. We also used the fact that the Wightman functions are even in frequency and rotationally invariant. As noted in Ref [11, 10], Eq.4.11 has the form of a kinetic theory Boltzmann equation. This analogy inspires the ansatz that “particle” density at $-\mathbf{p}$ is equals “hole” density at \mathbf{p} , that is $g_+(-\mathbf{p}) = g_-(\mathbf{p})$. This finally allows us to decouple the two equations; we arrive at the following (dropping the homogeneous term) final expression:

$$\begin{aligned} (-i\nu + i\mathbf{q} \cdot \mathbf{v}_{\mathbf{p}}) g_+(\mathbf{p}) = & \frac{1}{N} \int_{\mathbf{p}'} \left[\mathcal{R}_+(\mathbf{p}', \mathbf{p}) + \mathcal{R}_-(\mathbf{p}', \mathbf{p}) - 2N\Gamma_{\mathbf{p}}\delta^{(2)}(\mathbf{p}' - \mathbf{p}) \right] g_+(\mathbf{p}') \end{aligned} \quad (4.16)$$

Our identification of the Butterfly velocity following Eqn 4.5 holds assuming the eigenvectors $g_+(\mathbf{p})$ of the equation above are weakly \mathbf{q} dependent.

5. Numerical Results

We now describe the solution of 3.8 and 4.16. It is achieved by discretizing the momentum integral on the right hand side into a sum. This turns the integral kernel into a matrix and the function $g(\nu, \mathbf{q}; \mathbf{p}')$ into a vector. We diagonalize this matrix. Using eigenfunctions we simplify to the form 4.2 (or similar for $\mathbf{q} \neq 0$). Finally an inverse Laplace transform takes us to real time.

The numerical calculations were carried out as described below for $\alpha = 10^{-1}, 10^{-2}, 10^{-5}$:

- We were able to eliminate the Dirac delta functions present in $\Im \Pi_{\lambda,R}(\nu, \mathbf{q})$ by solving the quartic polynomial in the argument. This produced four integrals over two-dimensional momentum that nevertheless still vanish in some regions.
- We computed $\Im \Pi_{\lambda,R}(\nu, \mathbf{q})$ at fixed \mathbf{q} for many values of ν , particularly densely around $\nu_*(\mathbf{q}) = \sqrt{\alpha \mathbf{q}^2 + \kappa \mathbf{q}^4}$.
- We rescaled the ν coordinate of these slices by $\nu_*(\mathbf{q})$ and interpolated linearly between them (in the \mathbf{q} direction).
- We performed the Kramers-Kronig transform as outlined in Appendix D.
- We computed A_λ from $\mathcal{G}_{R,\lambda}$ and from this obtained the \mathcal{R}_1 functions.
- To obtain \mathcal{R}_2 we performed yet another momentum integral with the same delta function solution as earlier. This function depends on four independent real parameters (frequency, two momentum magnitudes, a relative angle) and therefore cannot be precomputed and stored for later fast lookup.
- For the $\mathbf{q} = 0$ case we discretized the integral equation of Eq.3.8 and turned it into an eigenvalue equation on an adaptively spaced grid of at least 60×60 , or as fine as necessary to achieve grid spacing independence of the result.
- For $\mathbf{q} \neq 0$ due to the lack of rotational invariance of Eq. 4.16 we are forced to use the separate components of the momentum, and which lead to much smaller grid sizes around 25×25 (still leading to matrices of roughly 8000×8000).

The total duration of our calculations was several thousand CPU hours. All our computations were performed with $\kappa = 1$. Furthermore, we chose to study OTO correlations only of current operators, $\nabla \phi$. The main result of this paper is the existence of a finite chaotic Lyapunov exponent for such operators; we express it in the form $\lambda_L = n(u, T) \frac{T}{N}$, where $n(u, T)$ is a dimensionless function that is either weakly dependent on or completely independent of temperature. We estimate an error margin of 50% on our results for $n(u, T)$. Recall that the ratio $\alpha = r_{\text{eff}}(u, T)/T$ is uniquely determined by T, κ, u, Λ . However, in light of its very weak dependence on temperature, we consider it an effective independent parameter in wide temperature ranges.

In the *low temperature regime* our data (Fig.7) suggests that λ_L is weakly dependent on α as it goes to zero, which corresponds to decreasing temperature. At large values of the interaction strength there does not appear to be a monotonic dependence of the Lyapunov exponent on α ; our numerical error estimates preclude us from resolving this.

This same figure can be interpreted instead in the *weak interaction regime* when $\alpha \sim u \log(u)$ is temperature independent. As expected chaos vanishes as $u \rightarrow 0$. The

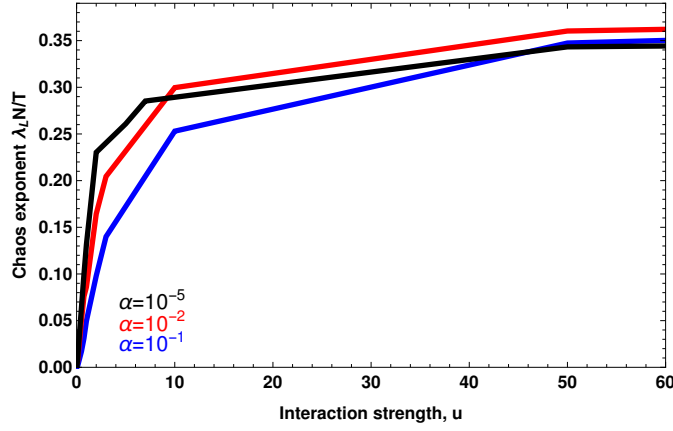


Figure 7. Lyapunov exponent at different temperatures as a function of interaction strength.

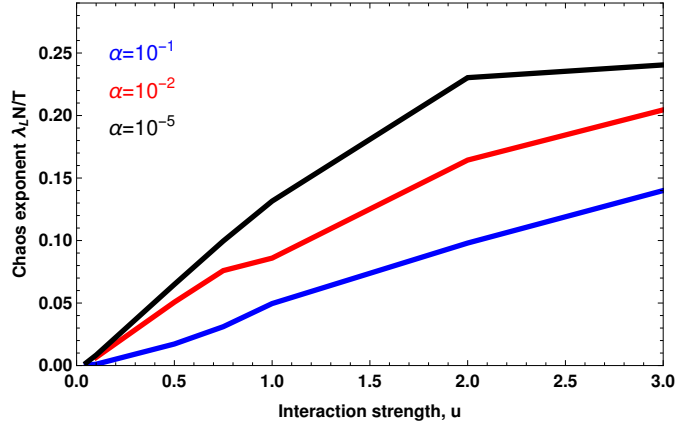


Figure 8. Lyapunov exponent at different temperatures at small interaction strength. The non-monotonicities are due to the inaccuracy of our numerical algorithm.

saturation of the chaotic exponent at large interaction strengths can be understood from the dressed propagator of the auxiliary field λ , (suppressing indices) of the form

$$\mathcal{G}_\lambda = \frac{1}{\frac{-1}{2u} - \Pi} \quad (5.1)$$

This is the only place in the calculation where the interaction strength enters

explicitly in this regime (the self-energy Π is interaction independent). The saturation of the chaos exponent then follows from the fact that fluctuations, captured by Π , dominate the bare propagator. An intuitive way to understand the saturation is to realize that as $u \rightarrow \infty$, field configurations with non-zero values of the current $\nabla\phi$ become energetically suppressed and therefore the dynamics become more constrained.

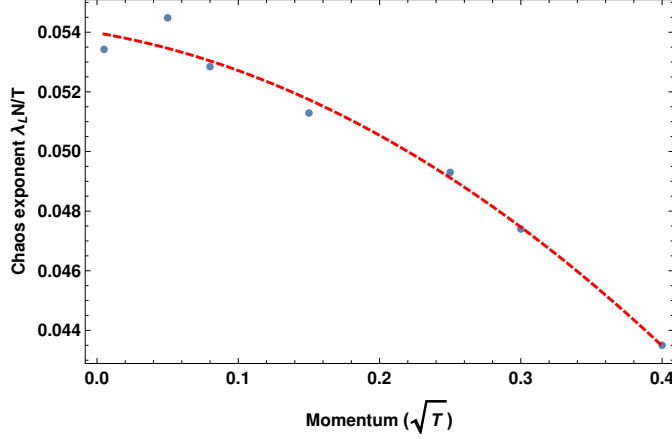


Figure 9. Lyapunov exponent $\lambda(\mathbf{k})$ vs momentum, in $C(t, \mathbf{k}) \sim \int d\mathbf{k} \exp(\lambda(\mathbf{k})t)$, at $\alpha = 0.1$ and $u = 1$. The fit gives $\lambda(\mathbf{k}) = 0.054 - 0.008k - 0.045k^2$, from which it follows that $v_B = 2\sqrt{0.054 \times 0.045}\sqrt{T} = 0.1\sqrt{T}$.

The two independent ways of computing λ_L (with $\mathbf{q} = 0$ and $\mathbf{q} \geq 0$) were within 50% of each other. Based on this we estimate our Butterfly velocities to have an error margin of about 50%. It is worth noting that the “thermal velocity” $\sqrt{r(T)} = \sqrt{\alpha(T)T}$ equals $\sqrt{0.1T} \approx 0.3\sqrt{T}$, which is larger than largest value of the Butterfly velocity of $0.23\sqrt{T}$ we obtained at $\alpha = 1, u = 2$. We did not compute the Butterfly velocity for values other than $\alpha = 0.1$ because the computations required more accuracy for small values of α and we estimated their running time to be impractically long.

6. Conclusions

We performed a perturbative calculation of a out-of-time-order correlator of current operators in the non-compact quantum Lifshitz model. We extracted the numerical values of the Lyapunov exponent and Butterfly velocity for a wide range of temperatures and/or interaction strengths. Our results indicate that the $(\nabla\phi)^4$ term is sufficient to generate chaos and is its dominant cause at sufficiently low energies. We observe that the Lyapunov exponent has a monotonic dependence on the interaction strength. In the *small temperature regime* it saturates at large values of interaction (which corresponds to the non-linear sigma model version of the quantum Lifshitz). In the *weak interaction regime* the Lyapunov exponent vanishes as the interaction strength vanishes. It is expected that for sufficiently generic interactions the Lyapunov

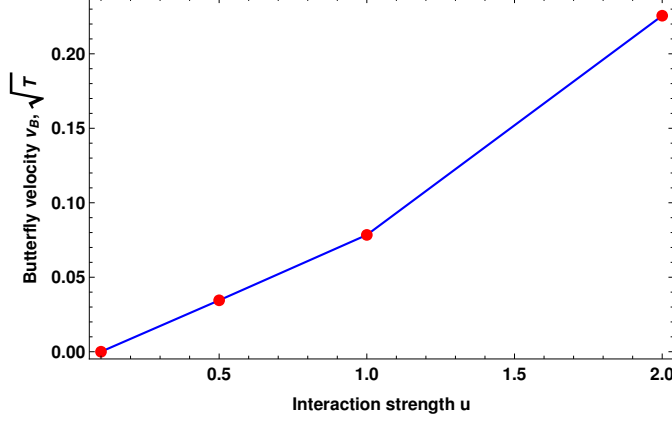


Figure 10. Butterfly velocity as a function of interaction strength at $\alpha = 0.1$.

exponent does not depend on the choice of operators in the OTO correlator. It would be interesting to verify this for our model, and for vertex operators in the compact version of qLM.

Acknowledgments

We thank Yuxuan Wang, Hart Goldman, Cristian Gaiđau, Thomas Scaffidi, and Juan Maldacena for discussions. We also thank Debanjan Chowdhury and Brian Swingle for making available their MATLAB code for the $O(N)$ model [11]. This work was supported in part by the Gordon and Betty Moore Foundation EPiQS Initiative through Grant No. GBMF4305 (EP) and by the National Science Foundation through the grant DMR 1725401 (EF).

Appendix A. Saddle-point solution at $N = \infty$

We rewrite Eq.1.11 in a form convenient for integrating out ϕ

$$S_{\phi, \lambda} = \frac{1}{2} \int d\tau_1 d^2 \mathbf{r}_1 d\tau_2 d^2 \mathbf{r}_2 \phi(\tau_1, x_1) G^{-1}(\tau_1, \mathbf{r}_1; \tau_2, \mathbf{r}_2) \phi(\tau_2, x_2) + \int d\tau d^2 \mathbf{r} \frac{\lambda^2(\tau, x)}{4u} \quad (\text{A.1})$$

where now

$$G^{-1}(\tau_1, x_1; \tau_2, x_2) = \delta(\tau_1 - \tau_2) \delta^{(2)}(\mathbf{r}_1 - \mathbf{r}_2) \times \left(-\partial_{\tau_1}^2 - r_{qc} \nabla_{\mathbf{r}_1}^2 + \kappa \nabla_{\mathbf{r}_1}^4 - \frac{1}{\sqrt{N}} \nabla \lambda(\tau_1, \mathbf{r}_1) \cdot \nabla - \frac{1}{\sqrt{N}} \lambda(\tau_1, \mathbf{r}_1) \nabla^2 \right) \quad (\text{A.2})$$

From now on we will write \mathbf{i} for the vector (τ_i, \mathbf{r}_i) in order to make things more readable.

We divide the ϕ_a into $N - 1$ components ϕ_\perp and π and we choose to integrate out ϕ_\perp and subsequently use the $\pi\pi$ correlations as a proxy for the $\phi\phi$ correlations of the original theory. At large N the difference between N and $N - 1$ is unimportant.

$$S_{\text{eff}}(\pi, \lambda) = \int d\tau d^2\mathbf{r} \frac{1}{2} \left[(\partial_\tau \pi)^2 + r_{qc} (\nabla \pi)^2 + \kappa (\nabla^2 \pi)^2 + \frac{\lambda(\tau, \mathbf{r})}{\sqrt{N}} (\nabla \pi)^2 \right] - \int d\tau d^2\mathbf{r} \frac{\lambda^2(\tau, x)}{4u} + \frac{N-1}{2} \ln \det G^{-1} \quad (\text{A.3})$$

The saddle-point equation for a spatially uniform λ is easiest found assuming all components of ϕ_a have been integrated out

$$\frac{\delta S_{\text{eff}}}{\delta \lambda} = 0 \quad (\text{A.4})$$

$$= -\beta L^2 \frac{2\lambda}{4u} + \frac{N}{2} \frac{\delta \ln \det G^{-1}}{\delta \lambda} \quad (\text{A.5})$$

$$= -\beta L^2 \frac{2\lambda}{4u} + \frac{\sqrt{N}}{2} \beta L^2 \frac{1}{\beta} \sum_{\omega_n} \int \frac{d^2\mathbf{q}}{(2\pi)^2} \frac{\mathbf{q}^2}{\omega_n^2 + (r_{qc} + \lambda/\sqrt{N})\mathbf{q}^2 + \kappa\mathbf{q}^4} \quad (\text{A.6})$$

Hence,

$$\lambda = u\sqrt{N} \frac{1}{\beta} \sum_{\omega_n} \int \frac{d^2\mathbf{q}}{(2\pi)^2} \frac{1}{\omega_n^2 + (r_{qc} + \lambda/\sqrt{N})\mathbf{q}^2 + \kappa\mathbf{q}^4} \quad (\text{A.7})$$

It will be convenient to define $r_{\text{eff}} = r_{qc} + \lambda/\sqrt{N}$ and replace λ in terms of it:

$$r_{\text{eff}} - r_{qc} = u \frac{1}{\beta} \sum_{\omega_n} \int \frac{d^2\mathbf{q}}{(2\pi)^2} \frac{\mathbf{q}^2}{\omega_n^2 + r_{\text{eff}}^2 \mathbf{q}^2 + \kappa\mathbf{q}^4} \quad (\text{A.8})$$

Using the identity

$$\frac{1}{\beta} \sum_{\omega_n} \frac{1}{\omega_n^2 + a^2} = \frac{1}{a} \left[\frac{1}{2} + \frac{1}{e^{\beta a} - 1} \right] \quad (\text{A.9})$$

we arrive at the final form of this self-consistent equation

$$r_{\text{eff}} - r_{qc} = u \int \frac{d^2\mathbf{q}}{(2\pi)^2} \frac{\mathbf{q}^2}{\sqrt{r_{\text{eff}} \mathbf{q}^2 + \kappa \mathbf{q}^4}} \left[\frac{1}{2} + \frac{1}{\exp\left(\beta \sqrt{r_{\text{eff}} \mathbf{q}^2 + \kappa \mathbf{q}^4}\right) - 1} \right] \quad (\text{A.10})$$

The physics is now most transparent. r_{eff} is the effective stiffness/velocity of the theory, and must vanish at the zero-temperature QCP. This implies r_{qc} must have the value

$$-r_{qc} = u \frac{1}{\beta} \sum_{\omega_n} \int \frac{d^2\mathbf{q}}{(2\pi)^2} \frac{\mathbf{q}^2}{\omega_n^2 + \kappa \mathbf{q}^4} = \frac{u}{8} \int_{\Lambda} \frac{d^2\mathbf{q}}{(2\pi)^2} \frac{\mathbf{q}^2}{\sqrt{\kappa \mathbf{q}^4}} \quad (\text{A.11})$$

which needs to be regularized with a UV cutoff.

It is difficult to solve Eq.A.10 directly, but it can be guessed that r_{eff} vanishes faster than T due to log corrections, and therefore in the regime where $r_{\text{eff}} \ll \sqrt{\kappa}T$ the equation becomes

$$r_{\text{eff}} = \frac{uT}{4\pi\kappa} \frac{\ln\left(\frac{\sqrt{\kappa}T}{r_{\text{eff}}}\right)}{1 + \frac{u}{16\pi\kappa^{3/2}} \left[\ln\left(\frac{4\kappa\Lambda^2}{r_{\text{eff}}}\right) \right]} \quad (\text{A.12})$$

When the log in the denominator dominates, and after rescaling $\bar{r} = r_{\text{eff}}/\sqrt{\kappa T}$, the equation simplifies to

$$\bar{r} = 4 \frac{\ln\left(\frac{1}{\bar{r}}\right)}{\ln\left(\frac{4\Lambda^2}{\bar{r}\sqrt{\kappa T}}\right)} = 4 \frac{\ln\left(\frac{1}{\bar{r}}\right)}{\ln\left(\frac{4\Lambda^2}{\sqrt{\kappa T}}\right) - \ln \bar{r}} \quad (\text{A.13})$$

The condition that in Eqn A.12 the denominator is dominated by the log implies in particular that $\bar{r} \ll \Lambda^2/\sqrt{\kappa T}$, which implies

$$\bar{r} \approx 4 \frac{\ln\left(\frac{1}{\bar{r}}\right)}{\ln\left(\frac{4\Lambda^2}{\sqrt{\kappa T}}\right)} \quad (\text{A.14})$$

Ignoring the log in the numerator we see that a putative solution to the equation is $\bar{r} = 4/\ln\left(\frac{4\Lambda^2}{\sqrt{\kappa T}}\right)$. We substitute it into the original equation and find that it is wrong by a prefactor $\ln\ln\left(\frac{4\Lambda^2}{\sqrt{\kappa T}}\right)$ which we incorporate into the new trial solution \bar{r} . Another substitution shows that the solution is now correct up to factors of $\left[\ln\ln\left(\frac{4\Lambda^2}{\sqrt{\kappa T}}\right)\right]^2 / \ln\left(\frac{4\Lambda^2}{\sqrt{\kappa T}}\right)^2 \approx \bar{r}^2$ which is guaranteed to be small because $\bar{r} \ll 1$.

Appendix B. $1/N$ corrections

Rewrite Eq.A.3 with the saddle-point solution substituted and simultaneously denote deviations from it by λ :

$$\begin{aligned} \frac{\lambda_{\text{sp}}}{\sqrt{N}} &= r_{\text{eff}} - r_{qc} \\ S_{\text{eff}}(\pi, \lambda_{\text{sp}} + \lambda) &= \int d\tau d^2\mathbf{r} \frac{1}{2} \left[(\partial_\tau \pi)^2 + r_{\text{eff}} (\nabla \pi)^2 + \kappa (\nabla^2 \pi)^2 + \frac{\lambda(\tau, \mathbf{r})}{\sqrt{N}} (\nabla \pi)^2 \right] \\ &\quad - \int d\tau d^2\mathbf{r} \frac{(\lambda_{\text{sp}} + \lambda)^2(\tau, x)}{4u} + \frac{N-1}{2} \ln \det G^{-1} \end{aligned}$$

where now

$$G^{-1}(1, 2) = \delta(1-2) \left(-\partial_1^2 - r_{\text{eff}} \nabla_1^2 + \kappa \nabla_1^4 - \frac{1}{\sqrt{N}} \nabla \lambda(1) \cdot \nabla_1 - \frac{1}{\sqrt{N}} \lambda(1) \nabla_1^2 \right) \quad (\text{B.1})$$

Now expand $\ln \det G^{-1}$ to second order in $\lambda(\tau, \mathbf{x})$ around the saddle-point value.

$$\ln \det G^{-1} = \text{tr} \ln G^{-1} \quad (\text{B.2})$$

$$= \text{tr} \ln G_0^{-1} (1 + G_0 B) = \text{tr} \ln G_0^{-1} + \text{tr} \ln (1 + G_0 B) \quad (\text{B.3})$$

$$= \text{tr} \ln G_0^{-1} + \text{tr} G_0 B - \frac{1}{2} \text{tr} (G_0 B)^2 + \dots \quad (\text{B.4})$$

The first order term will vanish when combined with the variation of the rest of the action due to the stationary phase condition. Finally, the second order term gives

$$G_0^{-1}(1, 2) = \delta(1-2) (-\partial_1^2 - r_{\text{eff}} \nabla_1^2 + \kappa \nabla_1^4) \quad (\text{B.5})$$

$$B(1, 2) = \frac{-1}{\sqrt{N}} \delta(1-2) [\nabla \lambda(1) \cdot \nabla + \lambda(1) \nabla^2] \quad (\text{B.6})$$

$$\text{tr} (G_0 B)^2 = \frac{1}{N} \int d1 d2 d3 d4 G_0(1, 2) B(2, 3) G_0(3, 4) B(4, 1) \quad (\text{B.7})$$

$$= \frac{1}{N} \int d1 d2 \lambda(1) \lambda(2) \nabla_1 \nabla_2 G_0(1, 2) \nabla_1 \nabla_2 G_0(2, 1) \quad (\text{B.8})$$

with which the effective action for λ at order $O(N^0)$ becomes

$$S_{\text{eff}}(\pi, \lambda) = \int d\tau d^2\mathbf{r} \frac{1}{2} \left[(\partial_\tau \pi)^2 + r_{\text{eff}} (\nabla \pi)^2 + \kappa (\nabla^2 \pi)^2 + \frac{\lambda(\tau, \mathbf{r})}{\sqrt{N}} (\nabla \pi)^2 \right] \\ - \frac{1}{\beta} \sum_{\omega_n} \int \frac{d^2\mathbf{q}}{(2\pi)^2} \lambda(\omega_n, \mathbf{q}) \lambda(-\omega_n, -\mathbf{q}) G_1^{-1}(i\omega_n, \mathbf{q}) \\ G_1^{-1}(i\omega_n, \mathbf{q}) = \left[-\frac{1}{4u} + \frac{1}{\beta} \sum_{\omega'_n} \int \frac{d^2\mathbf{p}}{(2\pi)^2} [(\mathbf{p} + \mathbf{q}) \cdot \mathbf{p}]^2 G_0(\omega'_n + \omega_n, \mathbf{p} + \mathbf{q}) G_0(\omega'_n, \mathbf{p}) \right]$$

Appendix C. Derivation of OTO rules

We work in the interacting picture, where the time-evolution operator is

$$U_I = \mathcal{T} \exp \left(\frac{i}{2\sqrt{N}} \sum_a \int_0^t ds \int_{\mathbf{x}} \lambda_0(\mathbf{x}, s) (\nabla \phi_a(\mathbf{x}, s))^2 \right) \quad (\text{C.1})$$

Its expansion looks like

$$U_I = 1 + \frac{i}{2\sqrt{N}} \sum_a \int_{s_1} \int_{\mathbf{x}} \lambda_0(\mathbf{x}, s) (\nabla \phi_a(\mathbf{x}, s))^2 \\ + \left(\frac{i}{2\sqrt{N}} \right)^2 \sum_{a,b} \int^t ds_1 \int^{s_1} ds_2 \int_{\mathbf{y}_1, \mathbf{y}_2} \lambda_0(\mathbf{y}_1, s_1) (\nabla \phi_a(\mathbf{y}_1, s_1))^2 \\ \times \lambda_0(\mathbf{y}_2, s_2) (\nabla \phi_b(\mathbf{y}_2, s_2))^2 \quad (\text{C.2})$$

We will need an expansion of $U_I^\dagger \phi_0(\mathbf{x}, t) U_I$, for which it will be useful to first establish a few identities:

$$[\lambda_0, \phi_0] = 0 \quad (\text{C.3})$$

$$[\phi_{0,a}(\mathbf{x}, t), \phi_{0,b}(0)] = i\mathcal{G}_R^{ab}(\mathbf{x}, t) \quad (\text{C.4})$$

$$[\phi_{0,a}(\mathbf{x}, t), \nabla \phi_{0,b}(\mathbf{y})] = \nabla_y i\mathcal{G}_R^{ab}(\mathbf{x} - \mathbf{y}, t) \quad (\text{C.5})$$

$$[\nabla \phi_{0,a}(\mathbf{x}, t), \nabla \phi_{0,b}(\mathbf{y})] = \nabla_x \nabla_y i\mathcal{G}_R^{ab}(\mathbf{x} - \mathbf{y}, t) \quad (\text{C.6})$$

$$[\phi_{0,a}(\mathbf{x}, t), (\nabla \phi_{0,b}(\mathbf{y}))^2] = 2 \nabla_y i\mathcal{G}_R^{ab}(\mathbf{x} - \mathbf{y}, t) \cdot \nabla_y \phi_{0,b}(\mathbf{y}) \quad (\text{C.7})$$

$$[\nabla \phi_{0,a}(\mathbf{x}, t), (\nabla \phi_{0,b}(\mathbf{y}))^2] = 2 \nabla_x \nabla_y i\mathcal{G}_R^{ab}(\mathbf{x} - \mathbf{y}, t) \cdot \nabla_y \phi_{0,b}(\mathbf{y}) \quad (\text{C.8})$$

$$(\text{C.9})$$

Finally, we got back to $U_I^\dagger \phi_0(\mathbf{x}, t) U_I$:

$$U_I^\dagger \phi_0(\mathbf{x}, t) U_I = \phi_0(\mathbf{x}, t) + \frac{i}{2\sqrt{N}} \sum_a \int^t ds \int_{\mathbf{y}} \left[\nabla \phi_0(\mathbf{x}, t), \lambda_0(\mathbf{y}, s) (\nabla \phi_{0,a}(\mathbf{y}, s))^2 \right] + \dots$$

Which means the first-order term in $C(t, \mathbf{x})$ is

$$C_1(t, \mathbf{x}_1 - \mathbf{x}_2) = \frac{-1}{N^2} \left(\frac{i}{2\sqrt{N}} \right)^2 \sum_{a,b,c,d} \int_{s_1, s_2} \int_{\mathbf{x}_1, \mathbf{x}_2} \\ \text{Tr} \{ \sqrt{\rho} \left[\left[\nabla \phi_a(\mathbf{x}_1, t), \lambda_0(\mathbf{y}_1, s_1) (\nabla \phi_{0,c}(\mathbf{y}_1, s_1))^2 \right], \nabla \phi_b(\mathbf{x}_2) \right] \right. \\ \left. \sqrt{\rho} \left[\left[\nabla \phi_a(\mathbf{x}_1, t), \lambda_0(\mathbf{y}_2, s_2) (\nabla \phi_{0,c}(\mathbf{y}_2, s_2))^2 \right], \nabla \phi_b(\mathbf{x}_2) \right] \right\}$$

$$\begin{aligned}
&= \frac{-1}{N^2} \left(\frac{i}{2\sqrt{N}} \right)^2 \sum_{a,b,c,d} \int_{s_1, s_2} \int_{\mathbf{x}_1, \mathbf{x}_2} \\
&\text{Tr}\{\rho \lambda_0(\mathbf{y}_1, s_1) \lambda_0(\mathbf{y}_2, s_2)\} 2 \nabla_x \nabla_y i \mathcal{G}_R^{ac}(\mathbf{x}_1 - \mathbf{y}_1, t - s_1) \cdot \nabla_y \nabla_x i \mathcal{G}^{cb}(\mathbf{y}_1 - \mathbf{x}_2, s_1) \\
&2 \nabla_x \nabla_y i \mathcal{G}_R^{ad}(\mathbf{x}_1 - \mathbf{y}_2, t - s_2) \cdot \nabla_y \nabla_x i \mathcal{G}^{db}(\mathbf{y}_2 - \mathbf{x}_2, s_2) \\
&= \frac{-1}{N^2} \left(\frac{i}{2\sqrt{N}} \right)^2 \sum_{a,b,c,d} \int_{s_1, s_2} \int_{\mathbf{x}_1, \mathbf{x}_2} \mathcal{G}_\lambda^W(\mathbf{y}_1 - \mathbf{y}_2, s_1 - s_2) \\
&2 \nabla_x \nabla_y i \mathcal{G}_R^{ac}(\mathbf{x}_1 - \mathbf{y}_1, t - s_1) \cdot \nabla_y \nabla_x i \mathcal{G}^{cb}(\mathbf{y}_1 - \mathbf{x}_2, s_1) \\
&2 \nabla_x \nabla_y i \mathcal{G}_R^{ad}(\mathbf{x}_1 - \mathbf{y}_2, t - s_2) \cdot \nabla_y \nabla_x i \mathcal{G}^{db}(\mathbf{y}_2 - \mathbf{x}_2, s_2)
\end{aligned}$$

Note that above the ∇_x and ∇_y are dotted with themselves. Another observation is that

$$\frac{1}{N^3} \sum_{abcd} \delta_{ac} \delta_{cb} \delta_{ad} \delta_{db} = \frac{1}{N^3} \sum_{ab} \delta_{ab} = \frac{1}{N^2} \quad (\text{C.10})$$

Finally, we Fourier transform and obtain:

$$\begin{aligned}
C_1(\nu) &= \int_t \int_{\mathbf{x}_1 - \mathbf{x}_2} C_1(t, \mathbf{x}_1 - \mathbf{x}_2) \\
&= \frac{1}{N^2} \int_{\mathbf{p}, \mathbf{p}'} (\mathbf{p} \cdot \mathbf{p}')^4 \int_{\omega, \omega'} \mathcal{G}_R(\mathbf{p}, \omega) \mathcal{G}_R(-\mathbf{p}, \nu - \omega) \\
&\quad \times \mathcal{G}_\lambda^W(\mathbf{p} - \mathbf{p}', \omega - \omega') \mathcal{G}_R(\mathbf{p}', \omega') \mathcal{G}_R(-\mathbf{p}', \nu - \omega') \quad (\text{C.11})
\end{aligned}$$

Had we chosen to instead dot product the gradient terms of ∇_{x_1} (and ∇_{x_2}) with ∇_{x_1} (and ∇_{x_2}) from other commutator, we would have had a different momentum-dependent numerator: $(\mathbf{p} \cdot \mathbf{p}')^2 \mathbf{p}^2 \mathbf{p}'^2$:

$$\begin{aligned}
C_1(\nu) &= \frac{1}{N^2} \int_{\mathbf{p}, \mathbf{p}'} \mathbf{p}^2 (\mathbf{p} \cdot \mathbf{p}')^2 \mathbf{p}'^2 \int_{\omega, \omega'} \mathcal{G}_R(\mathbf{p}, \omega) \mathcal{G}_R(-\mathbf{p}, \nu - \omega) \mathcal{G}_\lambda^W(\mathbf{p} - \mathbf{p}', \omega - \omega') \\
&\quad \times \mathcal{G}_R(\mathbf{p}', \omega') \mathcal{G}_R(-\mathbf{p}', \nu - \omega') \quad (\text{C.12})
\end{aligned}$$

Or generalized:

$$\begin{aligned}
C_{1(ijij)}(\nu, \mathbf{q}) &= \frac{1}{N^2} \int_{\mathbf{p}, \mathbf{p}'} \mathbf{p} \cdot (\mathbf{q} - \mathbf{p})(\mathbf{q} - \mathbf{p}) \cdot (\mathbf{q} - \mathbf{p}')(\mathbf{q} - \mathbf{p}') \cdot \mathbf{p}' \mathbf{p} \cdot \mathbf{p}' \quad (\text{C.13}) \\
&\quad \times \int_{\omega, \omega'} \mathcal{G}_R(\mathbf{p}, \omega) \mathcal{G}_R(-\mathbf{p}, \nu - \omega) \mathcal{G}_\lambda^W(\mathbf{p} - \mathbf{p}', \omega - \omega') \\
&\quad \times \mathcal{G}_R(\mathbf{p}', \omega') \mathcal{G}_R(-\mathbf{p}', \nu - \omega') \quad (\text{C.14})
\end{aligned}$$

This gives a diagram with one rung of Type 1. We can read off the Feynman rules from the above. They are:

- Draw a diagram
- Each line must be directed: left to right, and top to down. This determines whether a momentum/frequency is incoming or outgoing. The sum of incoming must equal sum of outgoing.
- Assign a value of $\frac{i \mathbf{k}_1 \cdot \mathbf{k}_2}{\sqrt{N}} \delta_{a,b}$ to each vertex, where the momenta belong to ϕ .
- Multiply overall diagram by $(\mathbf{k}_i \cdot \mathbf{k}_f)^2$ for C_{iijj} or $\mathbf{k}_i^2 \mathbf{k}_f^2$ for C_{ijij} , where the momenta $\mathbf{k}_i, \mathbf{k}_f$ emanate from \mathbf{x}_1 and \mathbf{x}_2 correspondingly.
- Retarded propagators for horizontal lines, Wightman for vertical.

To verify the rules for diagrams with Type 2 rungs we must expand $U_I^\dagger \phi U_I$ to second order.

$$\begin{aligned} \left[U_I^\dagger \phi_0(x, t) U_I \right]_2 &= \left(\frac{i}{2\sqrt{N}} \right)^2 \sum_{bc} \int_0^t ds_1 \int_0^{s_1} ds_2 \int_{\mathbf{y}_1, \mathbf{y}_2} \\ &\quad \left[\left[\phi_0(\mathbf{x}, t), \lambda_0(s_1, \mathbf{y}_1) (\nabla \phi_{0,b}(s_1, \mathbf{y}_1))^2 \right], \lambda_0(s_2, \mathbf{y}_2) (\nabla \phi_{0,c}(s_2, \mathbf{y}_2))^2 \right] \end{aligned}$$

The commutator in the term above becomes

$$\begin{aligned} [[,],] &= 2 \nabla_{y_1} i\mathcal{G}_R(\mathbf{x} - \mathbf{y}_1, t - s_1) \cdot \nabla_{y_1} \\ &\quad \times \nabla_{y_2} 2i\mathcal{G}_R(\mathbf{y}_1 - \mathbf{y}_2, s_1 - s_2) \cdot \nabla_{y_2} \phi(\mathbf{y}_2, s_2) \lambda(s_1) \lambda(s_2) \\ &\quad + 2 \nabla_{y_1} i\mathcal{G}_R(\mathbf{x} - \mathbf{y}_1, t - s_1) i\mathcal{G}_{R,\lambda}(\mathbf{y}_1 - \mathbf{y}_2, s_1 - s_2) (\nabla_y \phi(\mathbf{y}_2, s_2))^2 \nabla_{y_1} \phi(\mathbf{y}_1) \end{aligned}$$

where the ∇ 's of \mathbf{y}_1 are contracted amongst themselves, similarly for \mathbf{y}_2 .

Finally, we must actually consider $\left[\left[U_I^\dagger \phi_0(x_1, t) U_I \right]_2, \nabla_{x_2} \phi(x_2, 0) \right]$ on each time fold.

$$\begin{aligned} [[[,],], \nabla_{x_2} \phi(x_2, 0)] &= 2 \nabla_{y_1} i\mathcal{G}_R(\mathbf{x} - \mathbf{y}_1, t - s_1) \cdot \nabla_{y_1} \\ &\quad \times \nabla_{y_2} 2i\mathcal{G}_R(\mathbf{y}_1 - \mathbf{y}_2, s_1 - s_2) \cdot \nabla_{y_2} \\ &\quad \times \nabla_{x_2} i\mathcal{G}_R(\mathbf{y}_2 - \mathbf{x}_2, s_2) \lambda(s_1) \lambda(s_2) \\ &\quad + 2 \nabla_{y_1} i\mathcal{G}_R(\mathbf{x} - \mathbf{y}_1, t - s_1) i\mathcal{G}_{R,\lambda}(\mathbf{y}_1 - \mathbf{y}_2, s_1 - s_2) \\ &\quad \times \left[(\nabla_y \phi(\mathbf{y}_2, s_2))^2 \nabla_{y_1} \phi(\mathbf{y}_1), \nabla_{x_2} \phi(x_2, 0) \right] \end{aligned} \tag{C.15}$$

where

$$\begin{aligned} \left[(\nabla_y \phi(\mathbf{y}_2, s_2))^2 \nabla_{y_1} \phi(\mathbf{y}_1), \nabla_{x_2} \phi(x_2, 0) \right] &= \nabla_x \nabla_{y_1} i\mathcal{G}_R(\mathbf{y}_1 - \mathbf{x}_2, s_1) (\nabla_{y_2} \phi)^2 \\ &\quad + 2 \nabla_x \nabla_{y_2} i\mathcal{G}_R(\mathbf{y}_2 - \mathbf{x}_2, s_2) \cdot \nabla_{y_2} \phi(\mathbf{y}_2) \nabla_{y_1} \phi(\mathbf{y}_1) \end{aligned}$$

The first line in Eq.C.15 gives the diagram with two rungs of Type 1 (if the λ 's are contracted between the time folds), or a correction to the self-energy of ϕ . The second line can be verified to give a diagram with a single Type 2 rung, and a correction to the vertex (which is $1/N$ suppressed) in a Type 1 diagram. Furthermore, there are two types of Type 2 diagrams, ladder type, and crossed type. This latter is argued to be kinematically suppressed and is subsequently ignored.

Putting it all together, for a diagram with a single uncrossed Type 2 rung:

$$\begin{aligned} C_2(t, \mathbf{x}_1 - \mathbf{x}_2) &= \frac{-1}{N^2} \left(\frac{i}{2\sqrt{N}} \right)^4 \sum_{abcdef} \int_{s_1, s_2, s'_1, s'_2} \int_{\mathbf{y}_1, \mathbf{y}_2, \mathbf{y}'_1, \mathbf{y}'_2} \\ &\quad \times 2 \nabla_{x_1} \nabla_{y_1} i\mathcal{G}_R(\mathbf{x}_1 - \mathbf{y}_1, t - s_1) i\mathcal{G}_{R,\lambda}(\mathbf{y}_1 - \mathbf{y}_2, s_1 - s_2) \\ &\quad \times 2 \nabla_{x_2} \nabla_{y_2} i\mathcal{G}_R(\mathbf{y}_2 - \mathbf{x}_2, s_2) 2 \nabla_{x_1} \nabla_{y'_1} i\mathcal{G}_R(\mathbf{x}_1 - \mathbf{y}'_1, t - s'_1) \\ &\quad \times i\mathcal{G}_{R,\lambda}(\mathbf{y}_1 - \mathbf{y}'_2, s'_1 - s'_2) 2 \nabla_{x_2} \nabla_{y'_2} i\mathcal{G}_R(\mathbf{y}'_2 - \mathbf{x}_2, s'_2) \\ &\quad \times \nabla_{y_1} \nabla_{y'_1} \mathcal{G}_W(\mathbf{y}_1 - \mathbf{y}'_1, s_1 - s'_1) \nabla_{y_2} \nabla_{y'_2} \mathcal{G}_W(\mathbf{y}_2 - \mathbf{y}'_2, s_2 - s'_2) \end{aligned}$$

which in the end gives (with all factors of $i, 2, N$ upfront):

$$\begin{aligned} C_2(t, \mathbf{x}_1 - \mathbf{x}_2) &= \frac{1}{N^2} \int_{s_1, s_2, s'_1, s'_2} \int_{\mathbf{y}_1, \mathbf{y}_2, \mathbf{y}'_1, \mathbf{y}'_2} \\ &\quad \times \nabla_{x_1} \nabla_{y_1} \mathcal{G}_R(\mathbf{x}_1 - \mathbf{y}_1, t - s_1) \mathcal{G}_{R,\lambda}(\mathbf{y}_1 - \mathbf{y}_2, s_1 - s_2) \\ &\quad \times \nabla_{x_2} \nabla_{y_2} \mathcal{G}_R(\mathbf{y}_2 - \mathbf{x}_2, s_2) \nabla_{x_1} \nabla_{y'_1} \mathcal{G}_R(\mathbf{x}_1 - \mathbf{y}'_1, t - s'_1) \\ &\quad \times \mathcal{G}_{R,\lambda}(\mathbf{y}'_1 - \mathbf{y}'_2, s'_1 - s'_2) \nabla_{x_2} \nabla_{y'_2} \mathcal{G}_R(\mathbf{y}'_2 - \mathbf{x}_2, s'_2) \\ &\quad \nabla_{y_1} \nabla_{y'_1} \mathcal{G}_W(\mathbf{y}_1 - \mathbf{y}'_1, s_1 - s'_1) \nabla_{y_2} \nabla_{y'_2} \mathcal{G}_W(\mathbf{y}_2 - \mathbf{y}'_2, s_2 - s'_2) \end{aligned}$$

which in momentum space becomes

$$C_2(\nu) = \frac{1}{N^2} \int_{\mathbf{p}, \mathbf{p}', \mathbf{p}''} \int_{\omega, \omega', \omega''} (\mathbf{p} \cdot \mathbf{p}')^2 (\mathbf{p} \cdot (\mathbf{p}'' - \mathbf{p}))^2 (\mathbf{p}' \cdot (\mathbf{p}' - \mathbf{p}''))^2 \\ \times \mathcal{G}_R(\nu - \omega, -\mathbf{p}) \mathcal{G}_R(\omega, \mathbf{p}) \mathcal{G}_W(\omega'' - \omega, \mathbf{p}'' - \mathbf{p}) \\ \times \mathcal{G}_{R,\lambda}(\nu - \omega'', -\mathbf{p}'') \mathcal{G}_{R,\lambda}(\omega'', \mathbf{p}'') \mathcal{G}_R(\nu - \omega', -\mathbf{p}') \mathcal{G}_R(\omega', \mathbf{p}')$$

The $1/N$ counting follows from

$$\frac{1}{N^2} \left(\frac{1}{\sqrt{N}} \right)^4 \sum_{abcdef} \delta_{ac} \delta_{cd} \delta_{da} \delta_{be} \delta_{ef} \delta_{fb} = \frac{1}{N^2} \quad (\text{C.17})$$

such that we can write the diagram with one Type 2 rung as

$$C_{2(iiij)}(\nu) = \frac{1}{N^2} \int_{\mathbf{p}, \mathbf{p}'} (\mathbf{p} \cdot \mathbf{p}')^2 \int_{\omega, \omega'} \mathcal{G}_R(\nu - \omega, -\mathbf{p}) \mathcal{G}_R(\omega, \mathbf{p}) \mathcal{G}_{\text{eff}}(\omega', \omega, \mathbf{p}', \mathbf{p}) \\ \times \mathcal{G}_R(\nu - \omega', -\mathbf{p}') \mathcal{G}_R(\omega', \mathbf{p}') \quad (\text{C.18})$$

Compare it with

$$C_{1(iiij)}(\nu) = \frac{1}{N^2} \int_{\mathbf{p}, \mathbf{p}'} (\mathbf{p} \cdot \mathbf{p}')^4 \int_{\omega, \omega'} \mathcal{G}_R(\mathbf{p}, \omega) \mathcal{G}_R(-\mathbf{p}, \nu - \omega) \\ \times \mathcal{G}_\lambda^W(\mathbf{p} - \mathbf{p}', \omega - \omega') \mathcal{G}_R(\mathbf{p}', \omega') \mathcal{G}_R(-\mathbf{p}', \nu - \omega') \quad (\text{C.19})$$

we notice that replacing $(\mathbf{p} \cdot \mathbf{p}')^2 \mathcal{G}_\lambda^W(\mathbf{p}' - \mathbf{p}, \omega' - \omega)$ in C_1 by $(\mathbf{p} \cdot \mathbf{p}')^2 \mathcal{G}_\lambda^W(\mathbf{p}' - \mathbf{p}, \omega' - \omega) + \mathcal{G}_{\text{eff}}(\omega', \omega, \mathbf{p}', \mathbf{p})$ allows us to treat both one-rung diagrams simultaneously.

Recall that in defining the OTO correlator we had a choice in how to contract the spatial derivatives:

$$C_{ijkl}(t_1 - t_2, \mathbf{x}_1 - \mathbf{x}_2) = \frac{1}{N^2} \sum_{a,b} \text{Tr} \{ \sqrt{\rho} [\partial_i \phi_a(\mathbf{x}_1, t_1), \partial_j \phi_b(\mathbf{x}_2, t_2)]^\dagger \sqrt{\rho} [\partial_k \phi_a(\mathbf{x}_1, t_1), \partial_l \phi_b(\mathbf{x}_2, t_2)] \} \quad (\text{C.20})$$

N.B. So far we have worked with the contraction $C = \sum_{i,k} C_{iikk}$, but another choice is $C = \sum_{i,j} C_{ijij}$. I will work with the latter from now on due to certain simplifications.

Using the $ijij$ contraction:

$$C_{2(ijij)}(\nu) = \frac{1}{N^2} \int_{\mathbf{p}, \mathbf{p}'} \mathbf{p}^2 \cdot \mathbf{p}'^2 \int_{\omega, \omega'} \mathcal{G}_R(\nu - \omega, -\mathbf{p}) \mathcal{G}_R(\omega, \mathbf{p}) \\ \times \mathcal{G}_{\text{eff}}(\omega', \omega, \mathbf{p}', \mathbf{p}) \mathcal{G}_R(\nu - \omega', -\mathbf{p}') \mathcal{G}_R(\omega', \mathbf{p}') \quad (\text{C.21})$$

and

$$C_{1(ijij)}(\nu) = \frac{1}{N^2} \int_{\mathbf{p}, \mathbf{p}'} \mathbf{p}^2 (\mathbf{p} \cdot \mathbf{p}')^2 \mathbf{p}'^2 \int_{\omega, \omega'} \mathcal{G}_R(\mathbf{p}, \omega) \mathcal{G}_R(-\mathbf{p}, \nu - \omega) \\ \times \mathcal{G}_\lambda^W(\mathbf{p} - \mathbf{p}', \omega - \omega') \mathcal{G}_R(\mathbf{p}', \omega') \mathcal{G}_R(-\mathbf{p}', \nu - \omega') \quad (\text{C.22})$$

Or, in full generality:

$$C_{1(ijij)}(\nu, \mathbf{q}) = \frac{1}{N^2} \int_{\mathbf{p}, \mathbf{p}'} (\mathbf{q} - \mathbf{p}) \cdot \mathbf{p} (\mathbf{q} - \mathbf{p}') \cdot \mathbf{p}' \int_{\omega, \omega'} (\mathbf{q} - \mathbf{p}) \cdot (\mathbf{q} - \mathbf{p}') \mathbf{p} \cdot \mathbf{p}' \\ \times \mathcal{G}_R(\mathbf{p}, \omega) \mathcal{G}_R(-\mathbf{p}, \nu - \omega) \mathcal{G}_\lambda^W(\mathbf{p} - \mathbf{p}', \omega - \omega') \mathcal{G}_R(\mathbf{p}', \omega') \mathcal{G}_R(-\mathbf{p}', \nu - \omega') \quad (\text{C.23})$$

$$C_{2(ijij)}(\nu) = \frac{1}{N^2} \int_{\mathbf{p}, \mathbf{p}'} (\mathbf{q} - \mathbf{p}) \cdot \mathbf{p} (\mathbf{q} - \mathbf{p}') \cdot \mathbf{p}' \int_{\omega, \omega'} \mathcal{G}_R(\nu - \omega, -\mathbf{p}) \mathcal{G}_R(\omega, \mathbf{p}) \\ \mathcal{G}_{\text{eff}}(\omega', \omega, \mathbf{p}', \mathbf{p}; \mathbf{q}) \mathcal{G}_R(\nu - \omega', -\mathbf{p}') \mathcal{G}_R(\omega', \mathbf{p}') \quad (\text{C.24})$$

where now

$$\begin{aligned} \mathcal{G}_{\text{eff}}(\omega', \omega, \mathbf{p}', \mathbf{p}; \nu, \mathbf{q}) = \\ \int_{\mathbf{p}'', \omega''} (\mathbf{p}'' - \mathbf{p}) \cdot \mathbf{p} (\mathbf{q} - \mathbf{p}) \cdot (\mathbf{p}'' - \mathbf{p}) (\mathbf{q} - \mathbf{p}') \cdot (\mathbf{p}' - \mathbf{p}'') \mathbf{p}' \cdot (\mathbf{p}' - \mathbf{p}'') \\ \times \mathcal{G}_W(\omega'' - \omega, \mathbf{p}'' - \mathbf{p}) \mathcal{G}_W(\omega' - \omega'', \mathbf{p}' - \mathbf{p}'') \mathcal{G}_{R,\lambda}(\nu - \omega'', \mathbf{q} - \mathbf{p}'') \mathcal{G}_{R,\lambda}(\omega'', \mathbf{p}'') \end{aligned} \quad (\text{C.25})$$

NB. It really doesn't matter whether $\mathcal{G}_\lambda^W(\mathbf{p}' - \mathbf{p})$ or $\mathcal{G}_\lambda^W(\mathbf{p} - \mathbf{p}')$ is used. It amounts to a redefinition of momenta that keeps all other terms in C_1 the same. Therefore, it must be that $\mathcal{G}_\lambda^W(\mathbf{p}' - \mathbf{p}) = \mathcal{G}_\lambda^W(\mathbf{p} - \mathbf{p}')$

Appendix C.1. Crossed Diagrams

The first important observation comes from the Fourier space form of a Wightman correlator:

$$\mathcal{G}_W(\omega, \mathbf{q}) = \frac{A(\omega, \mathbf{q})}{2 \sinh\left(\frac{\beta\omega}{2}\right)} \quad (\text{C.26})$$

We see that in real time, $\mathcal{G}_W(t, \mathbf{r})$ has significant support only for $t \sim \beta^{-1}$. Now consider a ladder diagram of type 1 with two rungs. Its value is, schematically:

$$\begin{aligned} \chi_{\text{ladder}} = \int s_1 s_2 s'_1 s'_2 \mathcal{G}_R(t - s_1) \mathcal{G}_R(t - s'_1) \mathcal{G}_R(s_1 - s_2) \mathcal{G}_R(s'_1 - s'_2) \\ \times \mathcal{G}_{W,\lambda}(s_1 - s'_1) \mathcal{G}_{W,\lambda}(s_2 - s'_2) \mathcal{G}_R(s_2) \mathcal{G}_R(s'_2) \end{aligned} \quad (\text{C.27})$$

The retarded Green functions impose, in particular, $\theta(s_1 - s_2)\theta(s'_1 - s'_2)\theta(s_2)\theta(s'_2)$, while the Wightman function effectively imposes $s_1 - s'_1 \approx 0, s_2 - s'_2 \approx 0$. Putting them together the integration phase space is restricted to $\theta(s_1 - s_2)\theta(s_2)$.

Now compare this with the case of a crossed diagram

$$\begin{aligned} \chi_{\text{crossed}} = \int s_1 s_2 s'_1 s'_2 \mathcal{G}_R(t - s_1) \mathcal{G}_R(t - s'_1) \mathcal{G}_R(s_1 - s_2) \mathcal{G}_R(s'_1 - s'_2) \\ \times \mathcal{G}_{W,\lambda}(s_1 - s'_2) \mathcal{G}_{W,\lambda}(s'_1 - s_2) \mathcal{G}_R(s_2) \mathcal{G}_R(s'_2) \end{aligned} \quad (\text{C.28})$$

where the constraints are $\theta(s_1 - s_2)\theta(s'_1 - s'_2)\theta(s_2)\theta(s'_2)$, coming from the Green functions, and $s_1 - s'_2 \approx 0, s_2 - s'_1 \approx 0$ from the Wightman function. Together they require $\theta(s_1 - s_2)\theta(s_2 - s_1)$, to within β^{-1} .

That is why we conclude that the crossed diagrams are parametrically suppressed compared to the ladder diagrams, a fact important at late times.

Appendix C.2. Product of retarded Green functions

Let us extract the part of Eq.C.22 that contributes to the leading time dependence of $C(t)$. Define $f(\omega) = \mathcal{G}_\lambda^W(\mathbf{p}' - \mathbf{p}, \omega' - \omega)$. We first work with the free expressions for \mathcal{G}_R .

$$\begin{aligned} \mathcal{G}_R(\omega, \mathbf{k}) &= \frac{1}{(\omega + i0)^2 + \epsilon_{\mathbf{k}}^2} = \frac{1}{2\epsilon_{\mathbf{k}}} \left[\frac{1}{\omega - \epsilon_{\mathbf{k}} + i0} - \frac{1}{\omega + \epsilon_{\mathbf{k}} + i0} \right] \\ \mathcal{G}_R(\nu - \omega, -\mathbf{p}) \mathcal{G}_R(\omega, \mathbf{p}) &= \frac{1}{4\epsilon_{\mathbf{p}}^2} \left[\frac{1}{\nu - \omega - \epsilon_{\mathbf{p}} + i0} - \frac{1}{\nu - \omega + \epsilon_{\mathbf{p}} + i0} \right] \\ &\quad \times \left[\frac{1}{\omega - \epsilon_{\mathbf{p}} + i0} - \frac{1}{\omega + \epsilon_{\mathbf{p}} + i0} \right] \end{aligned}$$

$$\begin{aligned}
C_1(\nu) &\propto I(\omega') = \int \frac{d\omega}{2\pi} \mathcal{G}_R(\mathbf{p}, \omega) \mathcal{G}_R(-\mathbf{p}, \nu - \omega) f(\omega) \\
I(\omega') &= \frac{-i f(\omega = \nu - \epsilon_{\mathbf{p}})}{4\epsilon_{\mathbf{p}}^2} \left[\frac{1}{\nu - 2\epsilon_{\mathbf{p}} + i0} - \frac{1}{\nu + i0} \right] \\
&\quad + \frac{-i f(\omega = \nu + \epsilon_{\mathbf{p}})}{4\epsilon_{\mathbf{p}}^2} \left[\frac{1}{\nu + 2\epsilon_{\mathbf{p}} + i0} - \frac{1}{\nu + i0} \right]
\end{aligned}$$

NB. It is important that above $\mathcal{G}_{W,\lambda}(\omega' - \omega)$ not have any singularities in ω , otherwise we might get extra poles, or worse.

Now doing the ω' integral picking up the other poles, at $\omega' = \nu \pm \epsilon_{\mathbf{p}} + i0$:

$$\begin{aligned}
I_2(\nu, \mathbf{p}, \mathbf{p}') &= \int \frac{d\omega'}{2\pi} \mathcal{G}_R(\mathbf{p}', \omega') \mathcal{G}_R(-\mathbf{p}', \nu - \omega') I(\omega') \quad (\text{C.29}) \\
&= \frac{(-i)^2 \mathcal{G}_{W,\lambda}(\mathbf{p}' - \mathbf{p}, \nu - \epsilon_{\mathbf{p}'} - \nu + \epsilon_{\mathbf{p}})}{16\epsilon_{\mathbf{p}}^2 \epsilon_{\mathbf{p}'}^2} \\
&\quad \times \left[\frac{1}{\nu - 2\epsilon_{\mathbf{p}} + i0} - \frac{1}{\nu + i0} \right] \left[\frac{1}{\nu - 2\epsilon_{\mathbf{p}'} + i0} - \frac{1}{\nu + i0} \right] \\
&\quad + \frac{(-i)^2 \mathcal{G}_{W,\lambda}(\mathbf{p}' - \mathbf{p}, \nu + \epsilon_{\mathbf{p}'} - \nu - \epsilon_{\mathbf{p}})}{16\epsilon_{\mathbf{p}}^2 \epsilon_{\mathbf{p}'}^2} \\
&\quad \times \left[\frac{1}{\nu + 2\epsilon_{\mathbf{p}} + i0} - \frac{1}{\nu + i0} \right] \left[\frac{1}{\nu + 2\epsilon_{\mathbf{p}'} + i0} - \frac{1}{\nu + i0} \right] \quad (\text{C.30})
\end{aligned}$$

We must now consider the three kinds of poles in ν that are important for the inverse Laplace transform to $C(t)$: ν^{-2} , $\nu^{-1}(\nu \pm 2\epsilon_{\mathbf{p}})^{-1}$, $(\nu \pm 2\epsilon_{\mathbf{p}})^{-1}(\nu \pm 2\epsilon_{\mathbf{p}'})^{-1}$. The ν integral will be done above all singularities of $I_2(\nu, \mathbf{p}, \mathbf{p}')$ in the complex plane

$$\begin{aligned}
C(t > 0)_{(1)} &= \frac{-1}{N^2} \int \frac{d\nu}{2\pi} e^{-i\nu t} \frac{1}{(\nu + i0)^2} \int_{\mathbf{p}, \mathbf{p}'} (\mathbf{p} \cdot \mathbf{p}')^4 \\
&\quad \times \frac{\mathcal{G}_{W,\lambda}(\mathbf{p}' - \mathbf{p}, \epsilon_{\mathbf{p}'} - \epsilon_{\mathbf{p}}) + \mathcal{G}_{W,\lambda}(\mathbf{p}' - \mathbf{p}, \epsilon_{\mathbf{p}} - \epsilon_{\mathbf{p}'})}{16\epsilon_{\mathbf{p}}^2 \epsilon_{\mathbf{p}'}^2} \\
&= \frac{t}{N^2} \int_{\mathbf{p}, \mathbf{p}'} (\mathbf{p} \cdot \mathbf{p}')^4 \frac{\mathcal{G}_{W,\lambda}(\mathbf{p}' - \mathbf{p}, \epsilon_{\mathbf{p}'} - \epsilon_{\mathbf{p}}) + \mathcal{G}_{W,\lambda}(\mathbf{p}' - \mathbf{p}, \epsilon_{\mathbf{p}} - \epsilon_{\mathbf{p}'})}{16\epsilon_{\mathbf{p}}^2 \epsilon_{\mathbf{p}'}^2}
\end{aligned}$$

and

$$\begin{aligned}
C(t > 0)_{(2)} &= \frac{1}{N^2} \int_{\mathbf{p}, \mathbf{p}'} \int \frac{d\nu}{2\pi} e^{-i\nu t} \frac{1}{(\nu + i0)(\nu - 2\epsilon_{\mathbf{p}} + i0)} (\mathbf{p} \cdot \mathbf{p}')^4 \\
&\quad \times \frac{\mathcal{G}_{W,\lambda}(\mathbf{p}' - \mathbf{p}, \epsilon_{\mathbf{p}} - \epsilon_{\mathbf{p}'})}{16\epsilon_{\mathbf{p}}^2 \epsilon_{\mathbf{p}'}^2} + \dots \\
&= \frac{i}{N^2} \int_{\mathbf{p}, \mathbf{p}'} \frac{1 + e^{-i2\epsilon_{\mathbf{p}} t}}{2\epsilon_{\mathbf{p}}} (\mathbf{p} \cdot \mathbf{p}')^4 \frac{\mathcal{G}_{W,\lambda}(\mathbf{p}' - \mathbf{p}, \epsilon_{\mathbf{p}} - \epsilon_{\mathbf{p}'})}{16\epsilon_{\mathbf{p}}^2 \epsilon_{\mathbf{p}'}^2} + \dots
\end{aligned}$$

Clearly all poles besides ν^{-2} give subleading time dependence at late-times, and therefore we will ignore them, and use the simplifying form

$$\mathcal{G}_R(\nu - \omega, -\mathbf{p}) \mathcal{G}_R(\omega, \mathbf{p}) = \frac{\pi i}{2\epsilon_{\mathbf{p}}^2} \left(\frac{\delta(\omega - \nu + \epsilon_{\mathbf{p}})}{\nu + i0} + \frac{\delta(\omega - \nu - \epsilon_{\mathbf{p}})}{\nu + i0} \right) \quad (\text{C.31})$$

or because of the two delta functions, might as well

$$\mathcal{G}_R(\nu - \omega, -\mathbf{p})\mathcal{G}_R(\omega, \mathbf{p}) = \frac{\pi i}{2\epsilon_{\mathbf{p}}^2} \left(\frac{\delta(\omega + \epsilon_{\mathbf{p}})}{\nu + i0} + \frac{\delta(\omega - \epsilon_{\mathbf{p}})}{\nu + i0} \right) \quad (\text{C.32})$$

$$= \frac{\pi i}{\epsilon_{\mathbf{p}}} \frac{\delta(\omega^2 - \epsilon_{\mathbf{p}}^2)}{\nu + i0} \quad (\text{C.33})$$

Finally, anticipating a self-energy induced finite lifetime $\Gamma_{\mathbf{p}} = \Im[\Sigma_R(\epsilon_{\mathbf{p}}, \mathbf{p})]/2\epsilon_{\mathbf{p}}$ (see Eqn E.5):

$$\mathcal{G}_R(\nu - \omega, -\mathbf{p})\mathcal{G}_R(\omega, \mathbf{p}) = \frac{\pi i}{\epsilon_{\mathbf{p}}} \frac{\delta(\omega^2 - \epsilon_{\mathbf{p}}^2)}{\nu + i2\Gamma_{\mathbf{p}}} \quad (\text{C.34})$$

Appendix C.3. Simplifying \mathcal{G}_{eff}

To include the contribution of the type 2 rungs we must simplify \mathcal{G}_{eff} first. In what follows we use the free ϕ field expressions for \mathcal{G}_W based on the observation that the self-energy $\Sigma_R \propto \frac{1}{N}$. It can be verified that:

$$\mathcal{G}_W(\omega, \mathbf{k}) = \mathcal{Q}(\omega)A(\omega, \mathbf{k}) \quad (\text{C.35})$$

$$\mathcal{Q}(\omega) = \frac{1}{2 \sinh\left(\frac{\beta\omega}{2}\right)} \quad (\text{C.36})$$

$$\mathcal{G}_W(\omega, \mathbf{k}) = \mathcal{Q}(\omega) \frac{\pi}{\epsilon_{\mathbf{k}}} (\delta(\omega - \epsilon_{\mathbf{k}}) - \delta(\omega + \epsilon_{\mathbf{k}})) \quad (\text{C.37})$$

Then

$$\begin{aligned} \mathcal{G}_W^2 &\equiv \mathcal{G}_W(\omega'' - \omega, \mathbf{p}'' - \mathbf{p})\mathcal{G}_W(\omega' - \omega'', \mathbf{p}' - \mathbf{p}'') \\ &= \frac{\pi^2 \mathcal{Q}(\omega'' - \omega)\mathcal{Q}(\omega' - \omega'')}{\epsilon_{\mathbf{p}'' - \mathbf{p}}\epsilon_{\mathbf{p}' - \mathbf{p}''}} [\delta(\omega'' - \omega - \epsilon_{\mathbf{p}'' - \mathbf{p}}) - \delta(\omega'' - \omega + \epsilon_{\mathbf{p}'' - \mathbf{p}})] \\ &\quad \times [\delta(\omega' - \omega'' - \epsilon_{\mathbf{p}' - \mathbf{p}''}) - \delta(\omega' - \omega'' + \epsilon_{\mathbf{p}' - \mathbf{p}''})] \end{aligned}$$

And after performing the ω'' integral and changing coordinates to $\bar{\mathbf{p}} = \mathbf{p}' - \mathbf{p}$, $\mathbf{P} = (\mathbf{p} + \mathbf{p}')/2$, $\bar{\omega} = \omega' - \omega$... we arrive at

$$\begin{aligned} \mathcal{G}_{\text{eff}}(\omega', \omega, \bar{\mathbf{p}}, \mathbf{P}) &= \frac{1}{2} \int \frac{d^2 \mathbf{p}''}{(2\pi)^2} \left[\left(\mathbf{P} - \frac{\bar{\mathbf{p}}}{2} \right) \cdot (\mathbf{p}'' + \frac{\bar{\mathbf{p}}}{2}) \left(\mathbf{P} + \frac{\bar{\mathbf{p}}}{2} \right) \cdot (\mathbf{p}'' - \frac{\bar{\mathbf{p}}}{2}) \right]^2 \frac{\pi}{\epsilon_+ \epsilon_-} \\ &\times \{ Q(\epsilon_+)Q(\bar{\omega} - \epsilon_+)\mathcal{G}_{R,\lambda}(\nu - \omega - \epsilon_+, -\mathbf{p}'' - \mathbf{P})\mathcal{G}_{R,\lambda}(\omega + \epsilon_+, \mathbf{p}'' + \mathbf{P}) (\delta(\bar{\omega} - \epsilon_+ - \epsilon_-) - \delta(\bar{\omega} - \epsilon_+ + \epsilon_-)) \\ &- Q(-\epsilon_+)Q(\bar{\omega} + \epsilon_+)\mathcal{G}_{R,\lambda}(\nu - \omega + \epsilon_+, -\mathbf{p}'' - \mathbf{P})\mathcal{G}_{R,\lambda}(\omega - \epsilon_+, \mathbf{p}'' + \mathbf{P}) (\delta(\bar{\omega} - \epsilon_+ - \epsilon_-) - \delta(\bar{\omega} + \epsilon_+ + \epsilon_-)) \} \end{aligned} \quad (\text{C.38})$$

Let θ (ϕ) be the angle between \mathbf{P} (\mathbf{p}'') and $\bar{\mathbf{p}}$, then

$$\begin{aligned} &\left[\left(\mathbf{P} - \frac{\bar{\mathbf{p}}}{2} \right) \cdot (\mathbf{p}'' + \frac{\bar{\mathbf{p}}}{2}) \left(\mathbf{P} + \frac{\bar{\mathbf{p}}}{2} \right) \cdot (\mathbf{p}'' - \frac{\bar{\mathbf{p}}}{2}) \right]^2 \\ &= \left[(Pp'' \cos(\theta - \phi) - \frac{\bar{p}^2}{4})^2 - \left(\frac{P\bar{p}}{2} \cos \theta - \frac{\bar{p}p''}{2} \cos \phi \right)^2 \right]^2 \end{aligned} \quad (\text{C.39})$$

For $\mathbf{q} \neq 0$, we can simplify to

$$\begin{aligned} \mathcal{G}_{\text{eff}}(\nu, \mathbf{q}; \omega, \omega', \mathbf{p}, \mathbf{p}') &= \frac{1}{2} \int \frac{d^2 \mathbf{p}''}{(2\pi)^2} \left[(\mathbf{q} - \mathbf{P} + \frac{\bar{\mathbf{p}}}{2}) \cdot (\mathbf{p}'' + \frac{\bar{\mathbf{p}}}{2}) (\mathbf{q} - \mathbf{P} - \frac{\bar{\mathbf{p}}}{2}) \cdot (\mathbf{p}'' - \frac{\bar{\mathbf{p}}}{2}) \right] \\ &\times \left[\left(\mathbf{P} - \frac{\bar{\mathbf{p}}}{2} \right) \cdot (\mathbf{p}'' + \frac{\bar{\mathbf{p}}}{2}) \left(\mathbf{P} + \frac{\bar{\mathbf{p}}}{2} \right) \cdot (\mathbf{p}'' - \frac{\bar{\mathbf{p}}}{2}) \right] \frac{\pi}{\epsilon_+ \epsilon_-} \end{aligned}$$

$$\begin{aligned} & \times \{Q(\epsilon_+)Q(\bar{\omega} - \epsilon_+)\mathcal{G}_{R,\lambda}(\nu - \omega - \epsilon_+, \mathbf{q} - \mathbf{p}'' - \mathbf{P})\mathcal{G}_{R,\lambda}(\omega + \epsilon_+, \mathbf{p}'' + \mathbf{P})(\delta(\bar{\omega} - \epsilon_+ - \epsilon_-) - \delta(\bar{\omega} - \epsilon_+ + \epsilon_-)) \\ & - Q(-\epsilon_+)Q(\bar{\omega} + \epsilon_+)\mathcal{G}_{R,\lambda}(\nu - \omega + \epsilon_+, \mathbf{q} - \mathbf{p}'' - \mathbf{P})\mathcal{G}_{R,\lambda}(\omega - \epsilon_+, \mathbf{p}'' + \mathbf{P})(\delta(\bar{\omega} - \epsilon_+ - \epsilon_-) - \delta(\bar{\omega} + \epsilon_+ + \epsilon_-))\} \end{aligned} \quad (\text{C.40})$$

Appendix D. λ self-energy

Appendix D.1. Zero temperature

$$\Pi(i\omega_n, \mathbf{q}) = \frac{1}{2} \int \frac{d\nu}{2\pi} \int_{\mathbf{k}}^{\Lambda} \frac{(\mathbf{k} \cdot (\mathbf{k} + \mathbf{q}))^2}{(\omega_n + \nu)^2 + \epsilon_{\mathbf{k}+\mathbf{q}}^2} \frac{1}{\nu^2 + \epsilon_{\mathbf{k}}^2} \quad (\text{D.1})$$

$$= \frac{1}{2} \int_{\mathbf{k}} (\mathbf{k} \cdot (\mathbf{k} + \mathbf{q}))^2 \frac{\epsilon_{\mathbf{k}} + \epsilon_{\mathbf{k}+\mathbf{q}}}{2\epsilon_{\mathbf{k}}\epsilon_{\mathbf{k}+\mathbf{q}}((\epsilon_{\mathbf{k}} + \epsilon_{\mathbf{k}+\mathbf{q}})^2 + \omega_n^2)} \quad (\text{D.2})$$

$$\Pi_R(\omega, \mathbf{q}) = \Pi(i\omega = \omega + i0, \mathbf{q}) \quad (\text{D.3})$$

$$= \frac{1}{2} \int_{\mathbf{k}} (\mathbf{k} \cdot (\mathbf{k} + \mathbf{q}))^2 \frac{1}{4\epsilon_{\mathbf{k}}\epsilon_{\mathbf{k}+\mathbf{q}}} \left[\frac{1}{(\omega + \epsilon_{\mathbf{k}} + \epsilon_{\mathbf{q}+\mathbf{k}} + i\epsilon)} - \frac{1}{(\omega - \epsilon_{\mathbf{k}} - \epsilon_{\mathbf{q}+\mathbf{k}} + i\epsilon)} \right] \quad (\text{D.4})$$

$$\text{Im } \Pi_R(\omega, \mathbf{q}) = \frac{1}{8} \int_{\mathbf{k}} \frac{(\mathbf{k} \cdot (\mathbf{k} + \mathbf{q}))^2}{\epsilon_{\mathbf{k}}\epsilon_{\mathbf{k}+\mathbf{q}}} [-\pi\delta(\omega + \epsilon_{\mathbf{k}} + \epsilon_{\mathbf{q}+\mathbf{k}}) + \pi\delta(\omega - \epsilon_{\mathbf{k}} - \epsilon_{\mathbf{q}+\mathbf{k}})] \quad (\text{D.5})$$

$$\begin{aligned} &= \frac{1}{8} \int_{\mathbf{k}} \frac{((\mathbf{k} - \mathbf{q}/2) \cdot (\mathbf{k} + \mathbf{q}/2))^2}{\epsilon_{\mathbf{k}-\mathbf{q}/2}\epsilon_{\mathbf{k}+\mathbf{q}/2}} \\ &\times [-\pi\delta(\omega + \epsilon_{\mathbf{k}-\mathbf{q}/2} + \epsilon_{\mathbf{k}+\mathbf{q}/2}) + \pi\delta(\omega - \epsilon_{\mathbf{k}-\mathbf{q}/2} - \epsilon_{\mathbf{k}+\mathbf{q}/2})] \end{aligned} \quad (\text{D.6})$$

where in the last line we shifted $\mathbf{k} \rightarrow \mathbf{k} - \mathbf{q}/2$. Now, some simplifications. We work first with $\epsilon_{\mathbf{k}}^2 = \sqrt{\kappa}k^4$.

$$\epsilon_{\mathbf{k}+\mathbf{q}/2}\epsilon_{\mathbf{k}-\mathbf{q}/2} = \kappa \left(\mathbf{k}^2 + \frac{\mathbf{q}^2}{4} + kq \cos \phi \right) \left(\mathbf{k}^2 + \frac{\mathbf{q}^2}{4} - kq \cos \phi \right) \quad (\text{D.7})$$

$$= \kappa \left[\left(\mathbf{k}^2 + \frac{\mathbf{q}^2}{4} \right)^2 - k^2 q^2 \cos^2 \phi \right] \quad (\text{D.8})$$

$$\epsilon_{\mathbf{k}-\mathbf{q}/2} + \epsilon_{\mathbf{k}+\mathbf{q}/2} = \sqrt{\kappa} \left(2\mathbf{k}^2 + \frac{\mathbf{q}^2}{2} \right) \quad (\text{D.9})$$

$$((\mathbf{k} - \mathbf{q}/2) \cdot (\mathbf{k} + \mathbf{q}/2))^2 = \left(\mathbf{k}^2 - \frac{\mathbf{q}^2}{4} \right)^2 \quad (\text{D.10})$$

Since the imaginary part of Π_R is easily seen to be odd in ω , we choose to evaluate the $\omega > 0$ part.

$$\text{Im } \Pi_R(\omega > 0, \mathbf{q}) = \frac{1}{8} \int_{\mathbf{k}} \frac{((\mathbf{k} - \mathbf{q}/2) \cdot (\mathbf{k} + \mathbf{q}/2))^2}{\epsilon_{\mathbf{k}-\mathbf{q}/2}\epsilon_{\mathbf{k}+\mathbf{q}/2}} \pi\delta(\omega - \epsilon_{\mathbf{k}-\mathbf{q}/2} - \epsilon_{\mathbf{k}+\mathbf{q}/2}) \quad (\text{D.11})$$

$$= \frac{\pi}{8} \int \frac{d\phi k dk}{(2\pi)^2} \frac{\left(\mathbf{k}^2 - \frac{\mathbf{q}^2}{4} \right)^2 \delta(\omega - \sqrt{\kappa} \left(2\mathbf{k}^2 + \frac{\mathbf{q}^2}{2} \right))}{\kappa \left[\left(\mathbf{k}^2 + \frac{\mathbf{q}^2}{4} \right)^2 - k^2 q^2 \cos^2 \phi \right]} \quad (\text{D.12})$$

For $\omega \geq \sqrt{\kappa}q^2/2$ we have the (physical) root

$$k_r = + \sqrt{\frac{\omega - \sqrt{\kappa}q^2/2}{2\sqrt{\kappa}}} = \sqrt{\frac{\omega}{2\sqrt{\kappa}} - \frac{q^2}{4}}$$

Putting it all together, and recalling that $|\mathbf{k}| \leq \Lambda$:

$$\begin{aligned} \text{Im } \Pi_R(\omega > 0, \mathbf{q}) &= \frac{\pi}{8} \int \frac{d\phi}{(2\pi)^2} \frac{\left(k_r^2 - \frac{q^2}{4}\right)^2}{\kappa \left[\left(k_r^2 + \frac{q^2}{4}\right)^2 - k_r^2 q^2 \cos^2 \phi\right]} \frac{k_r}{|-4\sqrt{\kappa}k_r|} \\ &\times \theta(\Lambda - k_r) \theta\left(\omega - \frac{\sqrt{\kappa}q^2}{2}\right) \end{aligned} \quad (\text{D.13})$$

$$= \frac{\pi}{8} \int \frac{d\phi}{(2\pi)^2} \frac{\frac{1}{2^2} \left(\frac{\omega}{\sqrt{\kappa}} - q^2\right)^2}{\kappa \left[\left(k_r^2 + \frac{q^2}{4}\right)^2 - k_r^2 q^2 \cos^2 \phi\right]} \frac{1}{4\sqrt{\kappa}} \quad (\text{D.14})$$

$$= \frac{\pi}{2^7 \kappa^{3/2}} \left(\frac{\omega}{\sqrt{\kappa}} - q^2\right)^2 \int \frac{d\phi}{(2\pi)^2} \frac{1}{\left[\left(k_r^2 + \frac{q^2}{4}\right)^2 - k_r^2 q^2 \cos^2 \phi\right]} \quad (\text{D.15})$$

Doing the ϕ integral, we have

$$\text{Im } \Pi_R(\omega > 0, \mathbf{q}) = \frac{\pi}{32\kappa^{3/2}} \frac{1}{2^2} \frac{\left(\frac{\omega}{\sqrt{\kappa}} - q^2\right)^2}{(2\pi)^2} \frac{2\pi\theta(\Lambda - k_r) \theta\left(\omega - \frac{\sqrt{\kappa}q^2}{2}\right)}{\sqrt{\left(k_r^2 + \frac{q^2}{4}\right)^2 \left[\left(k_r^2 + \frac{q^2}{4}\right)^2 - k_r^2 q^2\right]}} \quad (\text{D.16})$$

$$= \frac{\pi}{32\kappa^{3/2}} \frac{1}{2^2} \left(\frac{\omega}{\sqrt{\kappa}} - q^2\right)^2 \frac{1}{(2\pi)^2} \frac{32\pi}{q^4 - 16k_r^4} \quad (\text{D.17})$$

$$= \frac{\pi}{32\kappa^{3/2}} \frac{1}{2^2} \left(\frac{\omega}{\sqrt{\kappa}} - q^2\right)^2 \frac{1}{(2\pi)^2} \frac{8\pi\kappa}{\omega(\omega - \sqrt{\kappa}q^2)} \quad (\text{D.18})$$

$$= \frac{\pi}{32\kappa^{3/2}} \frac{1}{2^2} \frac{1}{(2\pi)^2} \frac{8\pi}{\omega} (\omega - \sqrt{\kappa}q^2) \quad (\text{D.19})$$

$$(\text{D.20})$$

and finally

$$\text{Im } \Pi_R(\omega > 0, \mathbf{q}) = \frac{1}{64\kappa^{3/2}} \frac{(\omega - \sqrt{\kappa}q^2)}{\omega} \theta\left(\omega - \frac{\sqrt{\kappa}q^2}{2}\right) \theta\left(2\sqrt{\kappa}(\Lambda^2 + \frac{q^2}{4}) - \omega\right) \quad (\text{D.21})$$

Appendix D.2. Finite temperature

At $T > 0$, we have expressions similar to Appendix B of Chowdhury:

$$\begin{aligned} \Im [\Pi_R(\nu + i0, q)]_{\nu > 0} &= \frac{1}{2} \int_{\mathbf{k}}^{\Lambda} \frac{\pi (\mathbf{k} \cdot (\mathbf{k} + \mathbf{q}))^2}{4\epsilon_{\mathbf{k}} \epsilon_{\mathbf{k}+\mathbf{q}}} 2 [b(\epsilon_{\mathbf{k}+\mathbf{q}}) - b(\epsilon_{\mathbf{k}})] \delta(\nu + \epsilon_{\mathbf{k}+\mathbf{q}} - \epsilon_{\mathbf{k}}) \\ &+ \frac{1}{2} \int_{\mathbf{k}}^{\Lambda} \frac{\pi (\mathbf{k} \cdot (\mathbf{k} + \mathbf{q}))^2}{4\epsilon_{\mathbf{k}} \epsilon_{\mathbf{k}+\mathbf{q}}} [b(\epsilon_{\mathbf{k}+\mathbf{q}}) - b(-\epsilon_{\mathbf{k}})] \delta(\epsilon_{\mathbf{k}+\mathbf{q}} + \epsilon_{\mathbf{k}} - \nu) \end{aligned} \quad (\text{D.22})$$

So far this expression is general, and $\epsilon_{\mathbf{k}}$ could be the one-loop corrected dispersion. Note that if we set $\mathbf{q} = 0$ above we obtain:

$$\Im [\Pi_R(\nu + i0, q = 0)]_{\nu > 0} = \frac{1}{2} \int_{\mathbf{k}}^{\Lambda} \frac{\pi (\mathbf{k})^4}{4\epsilon_{\mathbf{k}}^2} [b(\epsilon_{\mathbf{k}}) - b(-\epsilon_{\mathbf{k}})] \delta(2\epsilon_{\mathbf{k}} - \nu) \quad (\text{D.23})$$

This can be finally simplified to:

$$\Im [\Pi_R(\nu + i0, q = 0)]_{\nu > 0} = \frac{b(\nu/2) - b(-\nu/2)}{16\nu\sqrt{r^2 + \kappa\nu^2}} \left(\frac{-r + \sqrt{r^2 + \kappa\nu^2}}{2\kappa} \right)^2 \theta(2\sqrt{\kappa}\Lambda^2 - \nu)$$

Now, at $T = 0$ we must set $r = 0$ and we obtain

$$\Im [\Pi_R(\nu + i0, q)]_{\nu > 0} = \frac{1}{64\kappa^{3/2}} (2\sqrt{\kappa}\Lambda^2 - \nu) \quad (\text{D.24})$$

Sending $\nu \rightarrow 0$ instead we have

$$\Im [\Pi_R(\nu, q = 0)] = \frac{T}{16\nu^2 r} \frac{\nu^4}{16r^2} = T \frac{\nu^2}{2^8 r^3} \quad (\text{D.25})$$

which implies that $\mathcal{G}_{W,\lambda}(\nu, q = 0) \rightarrow 0$ as $\nu \rightarrow 0$ because the $1/\sinh(\beta\nu)$ is overcome.

After shifting $\mathbf{k} \rightarrow \mathbf{k} - \mathbf{q}/2$, and $\epsilon_{\pm} = \epsilon_{\mathbf{k} \pm \mathbf{q}/2}$ in (D.22):

$$\begin{aligned} \Im [\Pi_R(\nu + i0, q)]_{\nu > 0} &= \frac{1}{2} \int_{\mathbf{k}} \frac{\pi (k^2 - q^2/4)^2}{4\epsilon_+ \epsilon_-} 2[b(\epsilon_+) - b(\epsilon_-)] \delta(\nu + \epsilon_+ - \epsilon_-) \\ &+ \frac{1}{2} \int_{\mathbf{k}} \frac{\pi (k^2 - q^2/4)^2}{4\epsilon_+ \epsilon_-} [b(\epsilon_+) - b(-\epsilon_-)] \delta(\epsilon_+ + \epsilon_- - \nu) \quad (\text{D.26}) \end{aligned}$$

$$\begin{aligned} &= \frac{\pi}{8} \int \frac{d\phi}{(2\pi)^2} \int k dk \frac{(k^2 - q^2/4)^2}{\epsilon_+ \epsilon_-} 2[b(\epsilon_+) - b(\epsilon_-)] \delta(\nu + \epsilon_+ - \epsilon_-) \\ &+ \frac{\pi}{8} \int \frac{d\phi}{(2\pi)^2} \int k dk \frac{(k^2 - q^2/4)^2}{\epsilon_+ \epsilon_-} [b(\epsilon_+) - b(-\epsilon_-)] \delta(\epsilon_+ + \epsilon_- - \nu) \\ &= \frac{\pi}{8} \frac{1}{(2\pi)^2} (I_1 + I_2) \quad (\text{D.27}) \end{aligned}$$

At finite temperature it is imperative that we use the full expression for $\epsilon_{\pm}^2 = r(T)k_{\pm}^2 + \kappa k_{\pm}^4$. Let us scale somethings out:

$$A(\nu, q, r, \kappa, T) = \Im \Pi_R(\nu, q, r, \kappa, T) \quad (\text{D.28})$$

$$= B\left(\frac{\nu}{T}, \frac{q}{\sqrt{T}}, \frac{r}{T}, \kappa\right) \quad (\text{D.29})$$

Since $r(T) = \alpha(T)T$, where α is dimensionless and very weakly dependent on T , we will just replace $r/T = \alpha \approx \text{const}$, but keeping in mind it is actually a function of temperature. We can do this once more with dimensionless κ :

$$A(\nu, q, r, \kappa, T) = B\left(\frac{\nu}{T}, \frac{q}{\sqrt{T}}, \alpha, \kappa\right) \quad (\text{D.30})$$

$$= \frac{1}{\kappa^{3/2}} C\left(\frac{\nu}{T}, \frac{q\kappa^{1/4}}{\sqrt{T}}, \frac{\alpha}{\sqrt{\kappa}}\right) \frac{\pi}{8} \frac{1}{(2\pi)^2} \quad (\text{D.31})$$

where finally

$$C(\nu, q, \alpha) = I_1(\nu, q, \alpha) + I_2(\nu, q, \alpha) \quad (\text{D.32})$$

So we need to evaluate two integrals where implicitly we have set $\kappa = 1, T = 1$ and $\alpha \ll 1$ a constant.

$$I_1(\nu, q, \alpha) = 2 \int_0^{2\pi} d\phi \int_0^\infty k dk \frac{(k^2 - q^2/4)^2}{\epsilon_+ \epsilon_-} [b(\epsilon_+) - b(\epsilon_-)] \delta(\nu + \epsilon_+ - \epsilon_-) \quad (\text{D.33})$$

$$I_2(\nu, q) = \int d\phi \int k dk \frac{(k^2 - q^2/4)^2}{\epsilon_+ \epsilon_-} [b(\epsilon_+) - b(-\epsilon_-)] \delta(\epsilon_+ + \epsilon_- - \nu) \quad (\text{D.34})$$

Some observations that are useful for testing numerics: $I_2 = 0$ for $q > q^*$ where q^* is a root of $2\epsilon_q = \nu$. Recall due to the factor of $\sinh(\beta\omega)$ in $\mathcal{G}_{W,\lambda}$ we only care about $\omega/T \sim 1$, and certainly not $\omega/T \gg 1$. We verified numerically that $\Im\Pi_R(\nu, \mathbf{q}) \rightarrow \frac{1}{64\kappa^{3/2}}$ for $\nu \gg T, \kappa\mathbf{q}^2$, which matches the $T = 0, \mathbf{q} = 0$ result.

Appendix D.3. $\Re\Pi_R$

The KK relation tells us that for a function analytic in the upper half plane (which implies its real-time version vanishes for $t < 0$), its real and imaginary parts can be determined from each other.

$$\Re\Pi_R(\nu, \mathbf{q}) = \frac{2}{\pi} P \int_0^\infty d\nu \frac{\omega \Im\Pi_R(\omega, \mathbf{q}) - \nu \Im\Pi_R(\nu, \mathbf{q})}{\omega^2 - \nu^2} \quad (\text{D.35})$$

Armed with $\Re\Pi_R(\nu, \mathbf{q})$ we have the $O(1)$ dressed λ propagator:

$$\mathcal{G}_\lambda(i\omega_n, \mathbf{q}) = \frac{1}{\frac{-1}{4v} - \Pi(i\omega_n, \mathbf{q})} \quad (\text{D.36})$$

$$\mathcal{G}_{R,\lambda}(\omega + i0, \mathbf{q}) = -\mathcal{G}_\lambda(i\omega_n = \omega + i0, \mathbf{q}) \quad (\text{D.37})$$

$$= \frac{1}{\frac{1}{4v} + \Pi_R(\omega, \mathbf{q})} \quad (\text{D.38})$$

From the $T = 0$ expression for $\Im\Pi_R(\nu, \mathbf{q})$ we can see that since $\Im\Pi_R(\nu, \mathbf{q}) \rightarrow \frac{1}{64\kappa^{3/2}}$ at large ν , we expect a logarithmic divergence in the KK transform.

Numerically, it can be handled as follows. Find a number c , such that at $\nu = c\nu_*(\mathbf{q})$, $\Im\Pi_R$ is sufficiently close to its asymptotic value. In our case, for $r(T) = 10^{-5}T$, this turns out to be $c \approx 2500$. Split the integral

$$\Re\Pi_R(\omega, \mathbf{q}) = \frac{2}{\pi} \int_0^{2500\nu_*(\mathbf{q})} d\nu \frac{\omega \Im\Pi_R(\omega, \mathbf{q}) - \nu \Im\Pi_R(\nu, \mathbf{q})}{\omega^2 - \nu^2} \quad (\text{D.39})$$

$$+ \frac{2}{\pi} \int_{2500\nu_*(\mathbf{q})}^E d\nu \frac{\omega \Im\Pi_R(\omega, \mathbf{q}) - \nu \Im\Pi_R(\nu, \mathbf{q})}{\omega^2 - \nu^2} \quad (\text{D.40})$$

The first line can be done numerically, while the second can be done analytically with the numerics-backed observation that the imaginary part of Π_R doesn't change much.

$$\Re\Pi_R(\omega, \mathbf{q}) = \frac{2}{\pi} \int_0^{2500\nu_*(\mathbf{q})} d\nu \frac{\omega \Im\Pi_R(\omega, \mathbf{q}) - \nu \Im\Pi_R(\nu, \mathbf{q})}{\omega^2 - \nu^2} \quad (\text{D.41})$$

$$- \frac{2}{\pi} \Im\Pi_R(\omega, \mathbf{q}) \text{Arctanh}\left(\frac{\omega}{2500\nu_*(\mathbf{q})}\right) \quad (\text{D.42})$$

$$+ \frac{1}{64\pi\kappa^{3/2}} \log\left|\frac{E^2 - \omega^2}{(2500\nu_*(\mathbf{q}))^2 - \omega^2}\right| \quad (\text{D.43})$$

In subsequent computations we drop the term in the last line above.

Appendix E. Scattering rate of ϕ

We need to evaluate $G_R(\omega, \mathbf{q})$, and more specifically

$$\Sigma(i\omega_n, \mathbf{q}) = \frac{T}{N} \sum_{i\nu_n} \int_{\mathbf{k}}^\Lambda (\mathbf{q} \cdot (\mathbf{q} + \mathbf{k}))^2 \mathcal{G}(i\omega_n + i\nu_n, \mathbf{q} + \mathbf{k}) \mathcal{G}_\lambda(i\nu_n, \mathbf{k})$$

Following the Chowdhury[11] we derive

$$\begin{aligned} \Im \Sigma_R(\omega + i0, \mathbf{q}) &= \frac{1}{N} \int_{\mathbf{k}}^{\Lambda} (\mathbf{q} \cdot \mathbf{k})^2 \frac{\sinh(\beta\omega/2)}{4\epsilon_{\mathbf{k}} \sinh(\beta\epsilon_{\mathbf{k}})/2} \\ &\times [\mathcal{G}_{W,\lambda}(\epsilon_{\mathbf{k}} - \omega, \mathbf{k} - \mathbf{q}) + \mathcal{G}_{W,\lambda}(-\epsilon_{\mathbf{k}} - \omega, \mathbf{k} - \mathbf{q})] \end{aligned} \quad (\text{E.2})$$

Written in rescaled variables

$$\begin{aligned} \Im \Sigma_R(\omega T, \mathbf{q}\sqrt{T}) &= \frac{T^2}{N} \int_{\mathbf{k}}^{\Lambda/\sqrt{T}} (\mathbf{q} \cdot \mathbf{k})^2 \frac{\sinh(\omega/2)}{4\epsilon_{\mathbf{k}} \sinh(\epsilon_{\mathbf{k}})/2} \\ &\times [\mathcal{G}_{W,\lambda}(\epsilon_{\mathbf{k}} - \omega, \mathbf{k} - \mathbf{q}) + \mathcal{G}_{W,\lambda}(-\epsilon_{\mathbf{k}} - \omega, \mathbf{k} - \mathbf{q})] \end{aligned} \quad (\text{E.3})$$

Some observations: At $T = 0$, $\Im \Pi_R$ is cutoff independent (see Eq.D.21), but $\Re \Pi_R$ is clearly cutoff dependent and goes like $\log \Lambda$ because $\Im \Pi_R(\nu, \mathbf{q}) \rightarrow \frac{1}{64\kappa^{3/2}}$ as $\nu \rightarrow \infty$. Since the location of the pole is a physical quantity, we imagine adding corresponding counterterms that keep the $\nu = \sqrt{r(T)\mathbf{k}^2 + \mathbf{k}^4}$ dispersion for ϕ once Π is used to compute corrections to \mathcal{G} . Therefore, the theory can be fixed such that $\mathcal{G}_{W,\lambda}$ is cutoff independent.

Proceeding further, we note that in Eq.E.3, the cutoff Λ can be safely sent to infinity.

Finally, assuming $\Sigma_R(\epsilon_{\mathbf{q}}, \mathbf{q})$ is smaller than $\epsilon_{\mathbf{q}}$ (always true for sufficiently large N) we define the inverse lifetime

$$\Gamma_{\mathbf{q}} = \frac{\Im \Sigma_R(\epsilon_{\mathbf{q}}, \mathbf{q})}{2\epsilon_{\mathbf{q}}} \quad (\text{E.4})$$

$$\begin{aligned} \Gamma(\mathbf{q}\sqrt{T}) &= \frac{T}{2N} \int_{\mathbf{k}}^{\Lambda/\sqrt{T}} (\mathbf{q} \cdot \mathbf{k})^2 \frac{\sinh(\omega/2)}{4\epsilon_{\mathbf{q}}\epsilon_{\mathbf{k}} \sinh(\epsilon_{\mathbf{k}})/2} \\ &\times [\mathcal{G}_{W,\lambda}(\epsilon_{\mathbf{k}} - \omega, \mathbf{k} - \mathbf{q}) + \mathcal{G}_{W,\lambda}(-\epsilon_{\mathbf{k}} - \omega, \mathbf{k} - \mathbf{q})] \end{aligned} \quad (\text{E.5})$$

- [1] Pavan Hosur, Xiao-Liang Qi, Daniel A. Roberts, and Beni Yoshida. Chaos in quantum channels. *Journal of High Energy Physics*, 2016(2):4, Feb 2016.
- [2] A. I. Larkin and Y. N. Ovchinnikov. Quasiclassical method in the theory of superconductivity. *ZhETF*, 28, June 1969.
- [3] Alexei Kitaev. Hidden correlations in the hawking radiation and thermal noise. *Talk given at the Fundamental Physics Prize Symposium*, 2014.
- [4] Stephen H. Shenker and Douglas Stanford. Black holes and the butterfly effect. *Journal of High Energy Physics*, 2014(3):67, Mar 2014.
- [5] Juan Maldacena, Stephen H. Shenker, and Douglas Stanford. A bound on chaos. *Journal of High Energy Physics*, 2016(8):106, Aug 2016.
- [6] V. I. Arnold and A. Avez. *Ergodic Problems of Classical Mechanics*. Benjamin, 1978.
- [7] J. Moser. *Stable and Random Motions in Dynamical Systems*. Princeton University Press, 1973.
- [8] Yasuhiro Sekino and L. Susskind. Fast Scramblers. *Journal of High Energy Physics*, 2008:065, 2008.
- [9] S. Sachdev and J. Ye. Gapless spin-fluid ground state in a random quantum heisenberg magnet. *Phys. Rev. Lett.*, 70, 1993.
- [10] Douglas Stanford. Many-body chaos at weak coupling. *Journal of High Energy Physics*, 2016(10):9, Oct 2016.
- [11] Debanjan Chowdhury and Brian Swingle. Onset of many-body chaos in the $o(n)$ model. *Phys. Rev. D*, 96:065005, Sep 2017.
- [12] Daniel A. Roberts and Douglas Stanford. Diagnosing chaos using four-point functions in two-dimensional conformal field theory. *Phys. Rev. Lett.*, 115:131603, Sep 2015.
- [13] Yingfei Gu and Xiao-Liang Qi. Fractional statistics and the butterfly effect. *Journal of High Energy Physics*, 2016(8):129, Aug 2016.
- [14] Yichen Huang, Yong-Liang Zhang, and Xie Chen. Out-of-time-ordered correlators in many-body localized systems. *Annalen der Physik*, 529(7):1600318–n/a, 2017. 1600318.

- [15] Rong-Qiang He and Zhong-Yi Lu. Characterizing many-body localization by out-of-time-ordered correlation. *Phys. Rev. B*, 95:054201, Feb 2017.
- [16] Brian Swingle and Debanjan Chowdhury. Slow scrambling in disordered quantum systems. *Phys. Rev. B*, 95:060201, Feb 2017.
- [17] E. Ardonne, P. Fendley, and E. Fradkin. Topological order and conformal quantum critical points. *Annals of Physics*, 310:493, 2004.
- [18] E. Fradkin, D. Huse, R. Moessner, V. Oganesyan, and S. L. Sondhi. On Bipartite Rokhsar-Kivelson points and Cantor Deconfinement. *Phys. Rev. B*, 69:224415, 2004.
- [19] J. M. Stéphan, S. Furukawa, G. Misguich, and V. Pasquier. Shannon and entanglement entropies of one and two-dimensional critical wave functions. *Phys. Rev. B*, 80:184421, 2009.
- [20] P. Ghaemi, A. Vishwanath, and T. Senthil. Finite-temperature properties of quantum Lifshitz transitions between valence-bond solid phases: An example of local quantum criticality. *Phys. Rev. B*, 72:024420, 2005.
- [21] Benjamin Hsu and Eduardo Fradkin. Dynamical stability of the quantum Lifshitz theory in 2+1 dimensions. *Phys. Rev. B*, 87:085102, Feb 2013.
- [22] C. Gogolin, M. P. Müller, and J. Eisert. Absence of thermalization in nonintegrable systems. *Phys. Rev. Lett.*, 106:040401, 2011.
- [23] T Prosen and M Robnik. Energy level statistics in the transition region between integrability and chaos. *Journal of Physics A: Mathematical and General*, 26(10):2371, 1993.
- [24] Subir Sachdev. *Quantum Phase Transitions*. Cambridge University Press, Cambridge, UK, 2007.
- [25] Subir Sachdev Sean A. Hartnoll, Andrew Lucas. Holographic Quantum Matter. *ArXiv: hep-th/1612.07324*, 2016.
- [26] S. Bravyi, M. B. Hastings, and F. Verstraete. Lieb-robinson bounds and the generation of correlations and topological quantum order. *Phys. Rev. Lett.*, 97:050401, Jul 2006.
- [27] Daniel A. Roberts, Douglas Stanford, and Leonard Susskind. Localized shocks. *Journal of High Energy Physics*, 2015(3), Mar 2015.
- [28] Stephen H. Shenker and Douglas Stanford. Multiple shocks. *Journal of High Energy Physics*, 2014(12):46, Dec 2014.
- [29] Daniel A. Roberts and Brian Swingle. Lieb-robinson bound and the butterfly effect in quantum field theories. *Phys. Rev. Lett.*, 117:091602, Aug 2016.
- [30] Aavishkar A. Patel, Debanjan Chowdhury, Subir Sachdev, and Brian Swingle. Quantum butterfly effect in weakly interacting diffusive metals. *Phys. Rev. X*, 7:031047, Sep 2017.